

An updated catalogue of giant radio sources

A. Kuźmicz,^{1,2,3*} M. Jamrozy,² K. Bronarska, K. Janda-Boczar² D. J. Saikia^{4,5,6}

¹Center for Theoretical Physics, Polish Academy of Sciences, Al. Lotników 32/46, 02-668 Warsaw, Poland

²Astronomical Observatory, Jagiellonian University, ul. Orla 171, 30-244 Krakow, Poland

³Queen Jadwiga Astronomical Observatory in Rzepiennik Biskupi, 33-163 Rzepiennik Strzyżewski, Poland

⁴Inter-University Centre for Astronomy and Astrophysics (IUCAA), Ganeshkhind, Pune 411 007, India

⁵NCRA, TIFR, Post Bag 3, Ganeshkhind, Pune 411 007, India

⁶Cotton University, Panbazar, Guwahati 781 001, India

Accepted August 10, 2018

ABSTRACT

We present a catalogue of 349 giant radio sources (GRSs including both galaxies and quasars). The database contains all giants known to date from the literature. These GRSs cover the redshift range of $0.016 < z < 3.22$ and include radio sources of projected linear sizes larger than 0.7 Mpc which extend up to 4.7 Mpc. We provide the principal parameters (i.e. exact position of the host in the sky, redshift, angular and projected linear size, red optical magnitude, radio morphology type, total radio flux density and luminosity) for all the sources as well as characteristics of the sample. Based on the distribution of GRSs in the sky we identify regions where there is a paucity of giants, so that future surveys for this type of objects could concentrate primarily in these fields. From the analysis presented here, we estimate a lower limit for the expected number of GRSs as about 2000, for the resolution and sensitivity limits of FIRST, NRAO VLA Sky Survey and Sloan Digital Sky Survey surveys. Compared with earlier compilations, there is a significant increase in the number of large giants with sizes > 2 Mpc as well as those at high redshifts with $z > 1$. We discuss aspects of their evolution and suggest that these are consistent with evolutionary models.

Key words: galaxies: active – galaxies: nuclei – galaxies: structure – quasars: general – radio continuum: galaxies

1 INTRODUCTION

The giant radio sources (GRSs) are defined as extragalactic radio sources, hosted by galaxies (giant radio galaxies; GRGs) or quasars (giant radio quasars; GRQs), for which the projected linear size of radio structure is larger than 0.7 Mpc¹ (assuming $H_0=71$ km/s/Mpc, $\Omega_M = 0.27$, $\Omega_{\text{vac}} = 0.73$). The first objects of this type to be found were 3C236 and DA240, identified by Willis, Strom & Wilson (1974), while the first sample of 53 GRSs compiled from the literature was published by Ishwara-Chandra & Saikia (1999). Since that time, the number of these relatively rare sources have been growing in number due to the all-sky surveys and the increasing amount of sensitive and good-quality radio and optical data. Many research groups searched for giants over the entire sky using modern radio surveys

like the Westerbork Northern Sky Survey (Rengelink et al. 1997) at 0.3 GHz, the Sydney University Molonglo Sky Survey (SUMSS, Bock, Large & Sadler 1999) at 0.8 GHz, the NRAO VLA Sky Survey (NVSS, Condon et al. 1998) and the Faint Images of the Radio Sky at Twenty-Centimeters (FIRST, Becker, White & Helfand 1995) at 1.4 GHz. The more recent samples by Schoenmakers et al. (2000a), Saripalli et al. (2005), Lara et al. (2001a), Machalski, Jamrozy & Zola (2001); Machalski et al. (2006); Machalski, Koziel-Wierzbowska & Jamrozy (2007), Kuźmicz & Jamrozy (2012) as well as Dabhade et al. (2017) and others have increased the number of known GRSs more than 6 times as compared to the sample of Ishwara-Chandra & Saikia (1999).

However, GRSs may not be easily recognizable if the surface brightness of the lobes is low. This could be the case for the less luminous GRSs with large angular sizes. Also, at high redshifts, where the inverse-Compton losses against the cosmic microwave background radiation are large, extended radio sources could have weak radio lobes (e.g. Konar et al. 2004). In these cases the hot-spots or lobes may not appear to be connected with the radio core, thereby making the de-

* E-mail: cygnus@oa.uj.edu.pl

¹ Many earlier authors, assuming $H_0=50$ km/s/Mpc, have used a lower limit of 1 Mpc as the defining size for GRSs. For the currently accepted cosmological parameters as given above, a limiting size of ~ 0.7 Mpc is appropriate.

tection of GRSs quite a challenging task. Due to all these reasons as well as the steep spectra of many GRSs, the new-generation radio interferometers such as the LOw-Frequency ARray ([van Haarlem et al. 2013](#)), the Murchison Widefield Array (MWA; [Lonsdale et al. 2009](#)), the Square Kilometre Array (SKA; [Carilli & Rawlings 2004](#)) or upgrades of existing low-frequency telescopes such as the Giant Metrewave Radio Telescope (GMRT; [Gupta et al. 2017](#)) should be of particular help in finding more of these objects.

From previous studies, it is still unclear why just a small fraction of radio sources reach such large sizes. Nevertheless, owing to the observations conducted in the last decade, our knowledge of the nature of GRSs has progressed significantly. These investigations focused on the role of the properties of the intergalactic medium (IGM; [Machalski et al. 2006](#); [Subrahmanyam et al. 2008](#); [Kuligowska et al. 2009](#)), the advanced age of the radio structures (e.g. [Mack et al. 1998](#); [Machalski, Jamrozy & Saikia 2009](#)), recurrent radio activity (e.g. [Subrahmanyam, Saripalli & Hunstead 1996](#); [Schoenmakers et al. 2000a](#); [Saikia & Jamrozy 2009](#); [Machalski et al. 2011](#)), and specific properties of the central active galactic nuclei (AGNs; e.g. black hole mass and accretion rate, [Kuźmicz & Jamrozy 2012](#)), as underlying reasons for their gigantic sizes. They revealed that GRSs are quite similar to radio sources with smaller radio structures, but significantly older. There is a trend for the spectral ages of radio galaxies to increase with linear size (e.g. [Murgia et al. 1999](#); [Parma, Murgia & Morganti 1999](#); [Murgia 2003](#); [Jamrozy et al. 2008](#)). However, there also exist small-sized radio galaxies with large ages ($\sim 10^8$ yr). [Murgia et al. \(2011\)](#) presented a study of five very aged radio galaxies with linear sizes of only about 100 kpc. Considering the IGM properties, it has been measured that in the vicinity of some GRSs the IGM density is lower (e.g. [Schoenmakers et al. 2000b](#); [Lara et al. 2000](#)), while we need to understand why we do observe giants at higher redshifts ($z > 1$) where the IGM density is actually higher than at present. Moreover, [Komberg & Pashchenko \(2009\)](#) have shown that there is no correlation between the radio source size and the density of galaxies in the neighbourhood. However, we still lack an unequivocal explanation for the giant sizes of some of these radio sources. It is obvious that GRSs are very interesting objects worth intensive research. Investigations of their properties are necessary to fully understand the processes responsible for the formation and evolution of radio sources in general.

Moreover, GRSs can be useful for cosmological studies. They can help in determining the IGM properties at different redshifts. A number of studies carried out during the last several years show that GRSs are a very valuable tool for investigating the large-scale structure of the Universe. Their large sizes provide an opportunity to probe the distribution of the Warm-Hot Intergalactic Medium (WHIM) in filaments of the large-scale structure of the Universe (e.g. [Malarecki et al. 2015, 2013](#); [Pirya et al. 2012](#); [Peng, Chen & Strom 2015](#)). These studies focus on searching interactions of radio lobes with the ambient medium revealed through asymmetries of radio structures and the distribution of neighbouring galaxies. It is believed that through these kinds of investigations it will be possible to find the ‘missing’ baryons predicted by the Big Bang theory ([Peng, Chen & Strom 2015](#)).

Furthermore, the recent investigations of [Bassani et al. \(2016\)](#) show that a large fraction of soft gamma-ray selected radio sources become GRSs. The all-sky observations of the INTEGRAL ([Winkler 1994](#)) and Swift ([Gehrels et al. 2004](#)) satellites reveal a large population of AGNs. The double-lobed radio sources are not too common in this group (about 7%), yet it is very intriguing that a large fraction of them are giants (23%). It may be the case that high-energy surveys could be more efficient in searching for new GRSs as compared to the radio surveys, where for example, in the well-studied 3CRR sample about 8% of the sources are identified as GRSs.

Given the above background, it is clear that it is highly advisable to look for new giants, and compiling a large sample of GRSs will facilitate future research in this field.

In this paper, we present a catalogue of GRSs known to date. We provide their principal parameters as well as characteristics of the sample. In this compilation of GRSs we do not consider objects such as cluster radio relics and/or radio halos that can also exceed our defining size of 700 kpc. The content of the paper is as follows. Section 2 describes details of the GRSs catalogue. In Sections 3 and 4 we analyse and discuss their distribution, physical parameters, and aspects of their evolution, while in Section 5 we present our concluding remarks.

2 CATALOGUE

For several years we have been browsing the literature, including survey results, and analysing data to search for radio galaxies of large linear sizes. We focused mostly on the existing compilations of giants, as well as published studies of individual sources of such types, but also examined well-studied samples such as 3CRR and compilations of structures of radio sources such as, for example, that by [Nilsson \(1998\)](#). In effect we have compiled a list of all GRSs known to the end of 2017. The list and principal parameters of GRSs are presented in Table 1 which is arranged as follows: Col. 1 – source name; Cols. 2 and 3 – J2000.0 coordinates of the GRS host galaxy or quasar; Col. 4 – optical identification (G – galaxy or Q – quasar); Col. 5 – redshift; Col. 6 – radio morphological type based on the Fanaroff-Riley classification scheme (see below); Col. 7 – angular size in arcmin; Col. 8 – projected linear size, D, in Mpc; Col. 9 – r band optical aperture magnitude; Col. 10 – total flux-density at 1.4 or 1.388 or 0.843 or 0.325 GHz in units of mJy; Col. 11 – error in total flux-density; Col. 12 – 1.4 GHz total radio luminosity in W/Hz; Col. 13 – References.

The redshifts enclosed within parentheses correspond to the photometric redshifts taken either from the literature or from the Sloan Digital Sky Survey (SDSS; [Albareti et al. 2017](#)). The 1.4 GHz flux-densities were measured mostly on the maps of the NVSS using the AIPS² software and particularly the task ‘tvstat’. During the measurements we have made efforts to exclude unrelated (foreground/background) sources superposed on the extent of some GRSs. For some

² www.aips.nrao.edu/index.shtml

sources with declination below -40° , we used the flux-density data at 1.388 GHz taken from [Saripalli et al. \(2012\)](#). They are marked as ‘*a*’ in the Table 1. The SUMSS flux-density measurements are marked as ‘*b*’, the measurements at 0.843 GHz given by [Saripalli et al. \(2005\)](#) are marked as letter ‘*c*’ and the measurements at 0.325 GHz given by [Sebastian et al. \(2018\)](#) are marked as letter ‘*d*’. In order to determine the flux-density error, we used the formula given by [Klein et al. \(2003\)](#):

$$\delta S = \sqrt{(S \cdot 0.03)^2 + (\sigma \cdot \sqrt{\frac{\Omega_{\text{int}}}{\Omega_{\text{beam}}}})^2}, \quad (1)$$

where ‘*S*’ is the measured total flux-density in mJy, the 0.03 value corresponds to the assumed 3% calibration error; ‘ σ ’ is the r.m.s. noise measured around the source, ‘ Ω_{int} ’ is the integration area, and ‘ Ω_{beam} ’ is the beam’s solid angle. The radio morphological type (FRI, FRII; [Fanaroff & Riley 1974](#)) was predominantly taken from the literature but for newly classified sources we judged it by ourselves using high-resolution radio maps. To determine the total radio luminosity, we used the formula given by [Brown, Webster & Boyle \(2001\)](#) and assumed for all sources a mean spectral index value as $\alpha = -0.8$ (following e.g. [Nilsson 1998](#)). For sources with only 0.843 or 0.325 GHz flux density measurements available we determined the 1.4 GHz flux density using the above given spectral index value.

For classical FRII sources, which constitute about 90 per cent of the sources in our list, we measure the angular extent as the size between the hotspots. Our measurements and those given by other authors are similar for these types of sources. In cases when we do not have an image of good enough angular resolution for a source, we adopt the angular size as was given in the literature. Controversies regarding angular size measurement appear mostly in the case of FRI (and hybrid FRI/FRII) sources. For such objects we try to estimate the angular size from a map/publication at which the source shows a maximal angular radio extent and its size was taken as the distance between the opposite edges. Something similar occurs for FRII sources (e.g. J0116–4722, J1548–3216) which show a double-double radio structure (without clear hotspots in the outer lobes) or those that have at least a clear extension beyond the hotspot(s) (e.g. DA240). In the case of sources which have a very curved morphology (e.g. wide-angle-tail, head tail radio galaxies) their angular extent was measured along the source ridge, and were not, as in the case of most giants, taken as the shortest distant between opposite edges.

The optical *r*-band aperture magnitudes are taken from the PanSTARRS data archive ([Flewelling et al. 2013](#)) which has surveyed the sky north of $\delta = -30^\circ$ in five photometric bands (*grizy*). For some objects south of $\delta = -30^\circ$ we have taken *r*-band magnitudes from [Saripalli et al. \(2012\)](#) and marked them as ‘*r*’ in Table 1.

The references given in Table 1 are mostly related to papers where a radio source has been recognised as a giant for the first time, or to papers where some important parameters characterising a particular object (e.g. redshift, radio map) were published. In Table 1 we include only the confirmed GRSs, though there are many more GRS candidates with redshifts still to be determined.

The final catalogue includes 349 sources, of which 280 are galaxies, 68 are quasars, and 1 is of uncer-

tain optical identification, covering the redshift range of $0.016 < z < 3.22$. In the sample, there are 46 objects with photometric estimation of redshifts. Redshifts larger than 1 were found for 22 GRSs based on spectroscopic measurements and for 6 GRSs based on photometric estimations. The most distant GRSs are J1145–0033 with redshift $z=2.055$ ([Kuźmicz, Kuligowska & Jamrozy 2011](#)) and J1235+3925 (i.e. 4C39.37) with redshift $z=3.22$ ([Mack et al. 2005](#)). However, the extent of the radio protrusions of the latter object is not certain, since [Mack et al. \(2005\)](#) mentioned that “it cannot be excluded that these are artefacts caused by an imperfect amplitude calibration”. Furthermore, 4C39.37 is the highest luminosity GRS in our sample. Although its structure needs to be confirmed, it is consistent with the extrapolation of the log $P - z$ relation (Figure 6) appearing as the most distant and luminous object.

More than half of the GRSs have projected linear sizes larger than 1 Mpc. Four of them have extremely large sizes: J1006+3454 (4.23 Mpc), J0931+3204 (4.29 Mpc), J1234+5318 (4.44 Mpc), J1420–0545 (4.69 Mpc). The last one is still the largest GRS known to date ([Machalski et al. 2008](#)). Most of the catalogued sources have an FRII radio morphology. Only 20 sources reveal an FRI structure and 16 are classified as hybrid FRI/FRII sources.

This sample of GRSs as a whole is quite heterogeneous, including objects from studies in which sources were not selected in any systematic manner. Moreover, it is restricted by the selection effects related to sensitivity of radio and optical surveys. However, it may be possible to construct statistically complete subsamples in restricted areas of the sky that have been imaged uniformly by surveys such as NVSS/FIRST and optical surveys such as SDSS.

3 SKY COVERAGE

In Figures 1 and 2 we plot the distributions of GRSs from our sample both in the Galactic and equatorial coordinates. It can be seen that it is not homogeneous and that a large fraction of known giants are seen in the northern hemisphere. On the sky maps there are regions where a lot of giants can be observed and regions without any recognized source (areas marked in gray in Figure 1). In the strip along the Galactic equator ($|b| \lesssim 15^\circ$), the optical identification of GRSs can be difficult due to higher Galactic extinction. Therefore, infrared surveys (e.g. the Two Micron All-Sky Survey; 2MASS; [Skrutskie et al. \(2006\)](#) or the Wide-field Infrared Survey Explorer (WISE; [Wright et al. \(2010\)](#)) can be helpful for identifying host galaxies in this region. Moreover, there are a number of extended individual radio structures inside the Milky Way Galaxy that may confuse some of the GRSs’ radio structure. The regions devoid of GRSs away from the Galactic plane are mostly due to incomplete coverage of both radio and optical surveys. Therefore, it would be good if future optical and radio survey efforts focus primarily on these ‘empty’ fields for identifications of new GRSs.

The largest number of giants is recognised in the regions that are covered by the FIRST radio survey, along with the availability of optical data (e.g. SDSS). As can be seen in Figure 2, where the surface density of giants in the sky plane is depicted by different colours, the densest region is located in the area defined by $12.8^{\text{h}} < \alpha < 14.4^{\text{h}}$ and

$36^\circ < \delta < 54^\circ$. There are 15 giants in this area, of which 12 are identified with galaxies and the remaining are identified with quasars. Similar numbers of GRGs are expected in other regions observed to similar radio and optical sensitivity limits. Extrapolating this density over the whole sky (4π sr) and assuming a homogeneous distribution of GRGs, the total number of giants should be about 2000. This estimate does not take into account objects with low surface brightness that remain undetectable in the NVSS survey. Also, since most of our sources have been selected from low-frequency surveys (less than about 1.4 GHz), core-dominated GRGs are also likely to be under-represented in the sample. Therefore, this is just a lower limit to the expected number of GRGs. Furthermore, the regions with the largest numbers of giants coincide with coverage of the FIRST survey, where better radio map resolution allowed for the identification of radio cores associated with host galaxies. However, it should be stressed that apart from regions that are not covered by both radio and optical surveys, there are also relatively large regions where FIRST and SDSS data are available but they still show a low number of GRGs. For example, such regions are placed near the North Galactic pole ($12^\text{h} < \alpha < 14.4^\text{h}$, $0^\circ < \delta < 18^\circ$ with density of only 2 GRGs over 317.33 deg^2) and in an area bounded by $21.8^\text{h} < \alpha < 3.6^\text{h}$, $0^\circ < \delta < 18^\circ$ (with an average density of 2.6 GRGs over 317.33 deg^2). The deficiency of known GRGs in those particular regions is not because of a lack of radio and optical data but due to a lack of conducting any systematic surveys for giants.

4 DISCUSSION

4.1 Physical parameters of the GRGs

In Figure 3, we present distributions of redshifts, projected linear sizes and 1.4 GHz total radio luminosities for the GRGs catalogued in this paper. The linear sizes range from the cut-off value of 700 kpc to 4.69 Mpc, with a median value of 1.14 Mpc. In the earlier compilation by Ishwara-Chandra & Saikia (1999) the largest source excluding 3C236, was 8C0821+695 which in our present cosmology has a projected linear size of 2.54 Mpc. In the present catalogue there are 13 sources with a size of at least 2.5 Mpc, a substantial increase that enable us to investigate the evolutionary status of these large sources. As seen in Figure 3 (middle panel), the FRII GRGs are mostly larger than the FRI GRGs. The median values of projected linear size of FRII, FRII/FRI and FRI type GRGs are 1.15, 1.18 and 0.99 Mpc, respectively. This indicates that the FRII radio sources tend to be larger than FRIs. Similar results were obtained by, e.g. Wing & Blanton (2011), who studied distributions of the projected linear size of the radio sources in clusters of galaxies.

There has also been a substantial increase in the number of high-redshift objects, say those with $z > 1$. The median redshift is 0.24 with the highest value being 3.22. There are 28 objects with a redshift of at least 1, while there were none in the earlier compilation by Ishwara-Chandra & Saikia (1999). Although a large number of larger sources at high redshifts have been discovered from the new, more sensitive surveys, most giants are relatively nearby objects with sizes close to 1 Mpc and 1.4 GHz total luminosity $\log P_{tot} [\text{W Hz}^{-1}]$

ranging from ~ 23.0 to 28.3 . The mean value of $\log P_{tot} [\text{W Hz}^{-1}] = 25.5$ for giants is slightly higher than the mean 1.4 GHz total radio luminosity of smaller sized FRII's (from the sample of Koziel-Wierzbowska & Stasińska 2011), which is equal to $\log P_{tot} [\text{W Hz}^{-1}] = 25.1$.

4.2 Hubble diagram for the GRGs

Although almost all the redshifts are spectroscopic, a few listed within brackets are photometric. Figure 4 shows the r -band apparent magnitude as a function of spectroscopic redshift, for the catalogued objects. This relation is known as the “Hubble diagram” and can be used to estimate the “photometric” redshift of galaxies lacking spectroscopic observations. Subsequently, we performed a linear regression fit to the PanSTARRS data points (excluding all objects with quasar hosts from this analysis), and obtained the following relation:

$$r_{mag} = (3.91 \pm 0.18) \log(z) + (21.11 \pm 0.15) \quad (2)$$

with a correlation coefficient of 0.89. Such a relation is consistent with the results obtained by Eales (1985) for a set of 3CRR galaxies, and suggests that the estimated redshifts are reasonably reliable. A similar relation but with a steeper slope, $r_{mag} = (8.83 \pm 0.35) \log(z) + (22.96 \pm 0.37)$ was obtained for 81 large angular sized radio galaxies by Lara et al. (2001b). The differences between our and Lara et al. (2001b) estimates are probably because of the different filter characteristics used during observations. For the low-redshift objects (mostly the brightest galaxies) the magnitudes from Lara et al. (2001b) are up to 3 mag brighter than those from PanSTARRS.

4.3 The luminosity–linear size (P–D) diagram

The radio luminosity–linear size (P–D) diagram has been used by many researchers in the past (e.g. Kaiser, Dennett-Thorpe & Alexander 1997; Ishwara-Chandra & Saikia 1999; Blundell, Rawlings & Willott 1999; Machalski, Chyží & Jamrozy 2004) as a useful tool to study the evolution of radio sources. In Figure 5 we plot the P–D relation for the sample of GRGs and smaller-sized 3CRR³ (Laing, Riley & Longair 1983) and FRII radio sources taken from Koziel-Wierzbowska & Stasińska (2011). We also superimpose the evolutionary tracks proposed by Kaiser, Dennett-Thorpe & Alexander (1997) for three different jet powers. For the 3CRR sample the flux densities measured at 0.178 GHz were extrapolated to the frequency of 1.4 GHz using the spectral index of individual sources and then the total radio luminosities were calculated using the formula given by Brown, Webster & Boyle (2001). Thirteen of the radio sources from the 3CRR sample, and 21 radio sources from the FRII sample have sizes larger than 0.7 Mpc; these are included in the sample of GRGs.

The models (e.g. Kaiser, Dennett-Thorpe & Alexander 1997; Ishwara-Chandra & Saikia 1999; Blundell, Rawlings & Willott 1999; Machalski, Chyží & Jamrozy 2004) all suggest that

³ <http://www.jb.man.ac.uk/atlas>

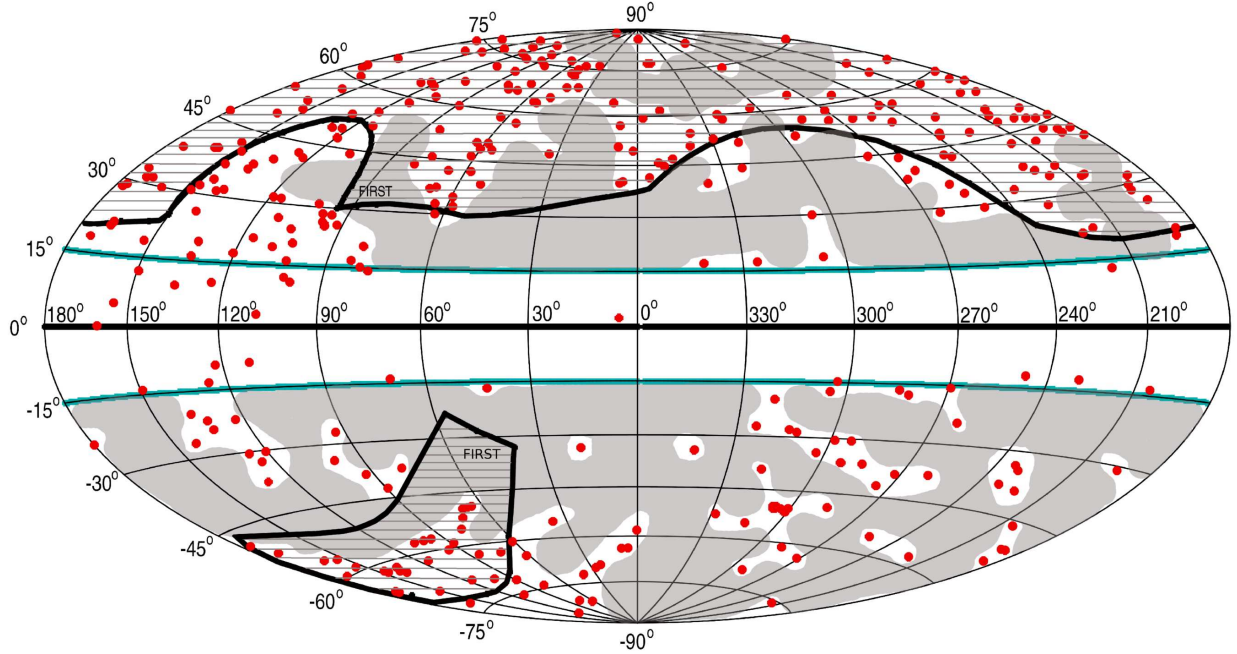


Figure 1. Distribution of GRSs in the plane of the sky in Galactic coordinates. The blue lines are plotted at Galactic latitudes $b=\pm 15^\circ$ denoting the larger Galactic extinction regions. In gray we coloured the regions outside the Galactic plane where no GRSs have been found. The sky area that is covered by the FIRST survey is framed by a thick black curve and in addition the area is hatched.

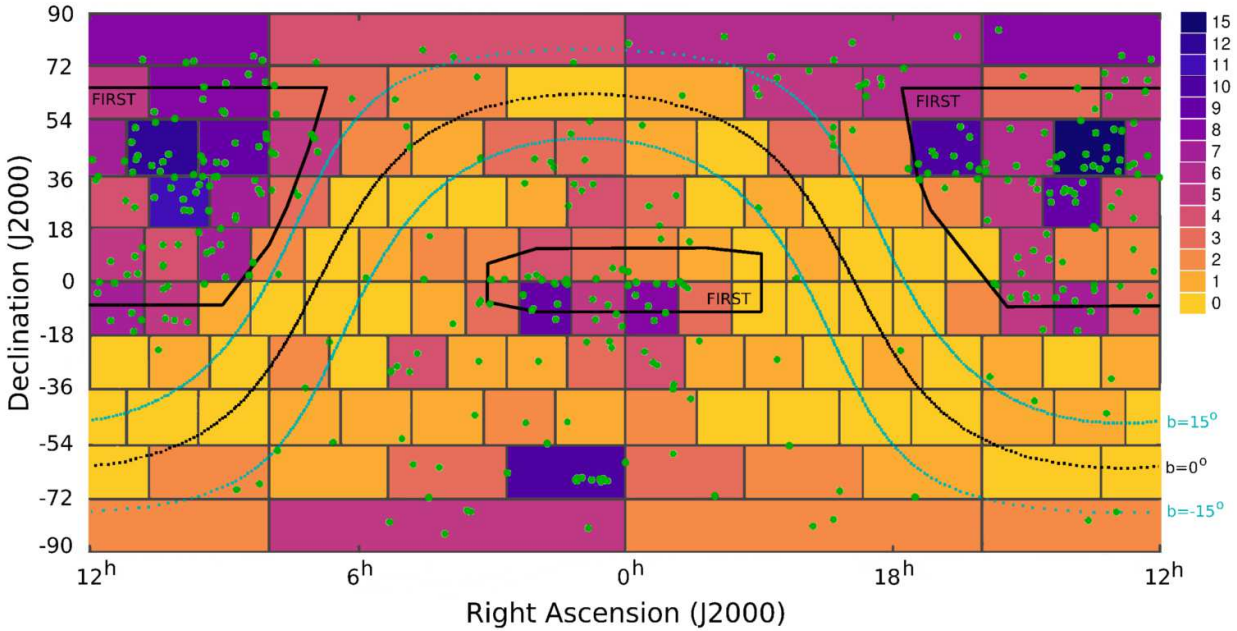


Figure 2. The distribution of GRSs in the plane of the sky in equatorial coordinates. The blue dotted lines correspond to the Galactic latitudes $b=\pm 15^\circ$ and the black dotted line corresponds to the Galactic equator. The different colours denote the number of giants counted inside a particular rectangle and every rectangle covers a the same area of 317.33 deg^2 (Malkin 2016).

the GRSs are the evolved counterparts of smaller, younger, and more luminous radio sources. The P–D diagram shows more clearly a declining upper envelope than was noted by Ishwara-Chandra & Saikia (1999). The lack of radio sources that have both large sizes and high radio luminosities

in our plot is consistent with model expectations of the evolution of radio sources. It has been postulated that GRSs evolve from normal FRII and FRI radio sources (e.g. Ishwara-Chandra & Saikia 1999), with sources of different jet powers following different evolutionary tracks in the P–D

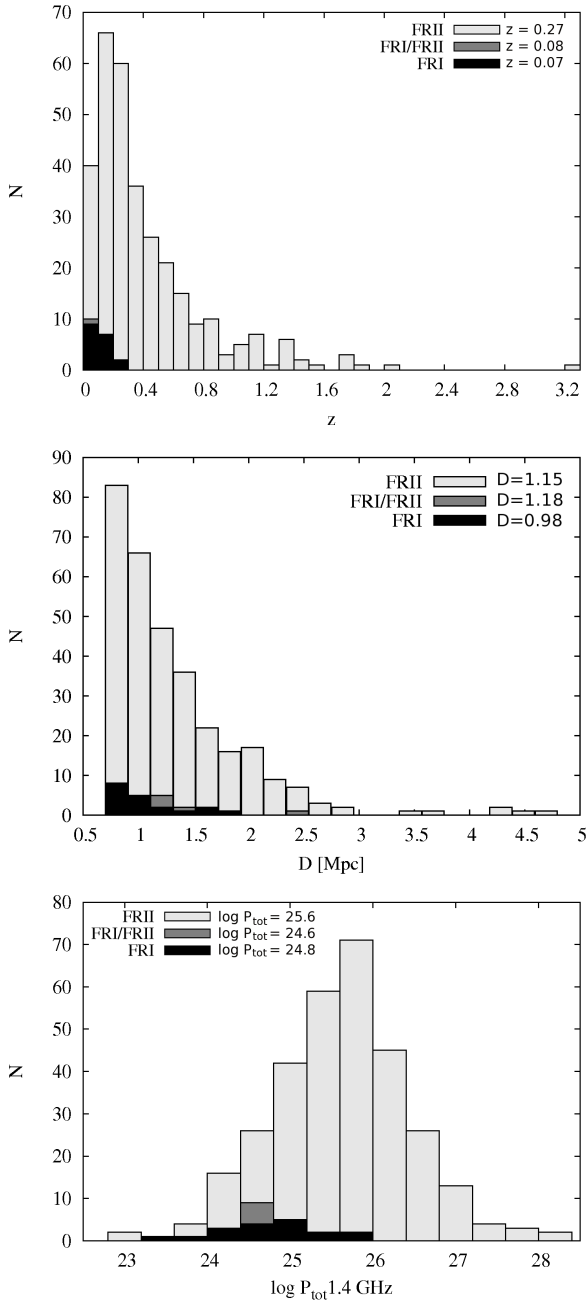


Figure 3. Distributions of redshift (top panel), projected linear size (middle panel), and 1.4 GHz total radio luminosity (bottom panel) for GRSSs. The number of sources N is put on the vertical axis. The values of redshift, projected linear size, and total radio luminosity given on the panels denote the median values for each morphological class of radio sources.

diagram. The upper envelope corresponds to a jet power of $\sim 10^{40}$ W. With the discovery of many high-redshift, luminous giant sources, the median value of total radio luminosities of the GRSSs, $\log P_{tot} [\text{W Hz}^{-1}] \sim 25.5$ is somewhat higher than that of typical FRII radio sources (from the sample of [Koziel-Wierzbowska & Stasińska 2011](#)) for which we obtained a median of $\log P_{tot} [\text{W Hz}^{-1}] = 25.1$. This fact, and evolutionary tracks from

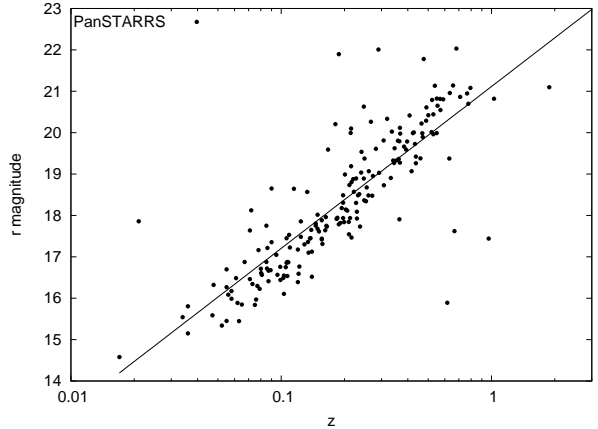


Figure 4. Correlation between r -band apparent PanSTARRS magnitude and redshift. The solid line corresponds to the best fit obtained for data points.

[Kaiser, Dennett-Thorpe & Alexander \(1997\)](#), indicate that the high-luminosity GRSSs evolve possibly from the most luminous radio sources like those from the 3CRR sample for which the median of $\log P_{tot} [\text{W Hz}^{-1}]$ is 26.4. Less-luminous GRSSs can evolve from lower-luminosity FRII and FRI radio sources. However, we observe the deficit of low-luminosity and high-redshift GRSSs visible in Figure 6 where we plot the total radio luminosity as a function of redshift, as would be expected in case of a Malmquist bias. However, in the P–D diagram (Figure 5) just as there appears to be a rough upper envelope for the GRSSs, the Figure 5 also suggests a rough lower envelope. The largest GRSSs are not of the lowest luminosities amongst the GRSSs. This apparent deficit of large, low-luminosity GRGs, is possibly due to a combination of selection effects (e.g. low surface-brightness of extended sources) and quenching due to inverse-Compton scattering.

4.4 High-redshift GRSSs

As noted earlier, there are 28 very distant GRSSs with redshift $z > 1$ in our sample. However, for a long time GRSSs were not expected to be found at high redshift. According to [Kapahi \(1989\)](#) since the density of the IGM increases as $\rho_{IGM} \propto (1+z)^3$, the radio lobe expansion could be significantly hampered at high redshifts. This explains the smaller median size (equal to 0.899 Mpc) of high-redshift giants in comparison with $z < 1$ GRSSs for which the median size is 1.16 Mpc. In addition, the surface brightness decreases with redshift as $(1+z)^{-4}$. This makes it difficult to recognise extended radio lobes and thus GRSSs themselves in earlier cosmological epochs. Nevertheless, the number of high-redshift GRSSs has grown due to sensitive radio surveys. We examine further the dependence of median size on redshift by considering equal number of GRSSs in each redshift bin, and also considering redshift bins of equal width (Figure 7). While in both cases there is a decrease in the median size with redshift for $z > 0.5$, the median size increases with redshift in the range $0 < z < 0.5$. Earlier studies of the linear size evolu-

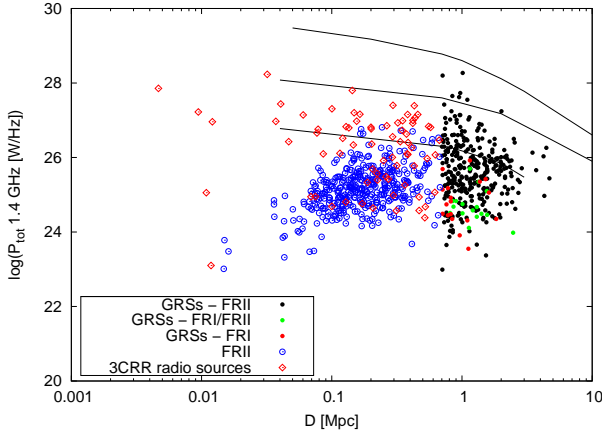


Figure 5. P–D diagram for GRSSs (dots), 3CRR radio sources (diamonds) from Laing, Riley & Longair (1983), and FRII radio sources from Koziel-Wierzbowska & Stasińska (2011) (pluses). The solid lines (from top to bottom) represent the evolutionary scenarios from Kaiser, Dennett-Thorpe & Alexander (1997) for jet powers of 1.3×10^{40} W at $z=2$, 1.3×10^{39} W at $z=0.5$ and 1.3×10^{38} W at $z=0.2$.

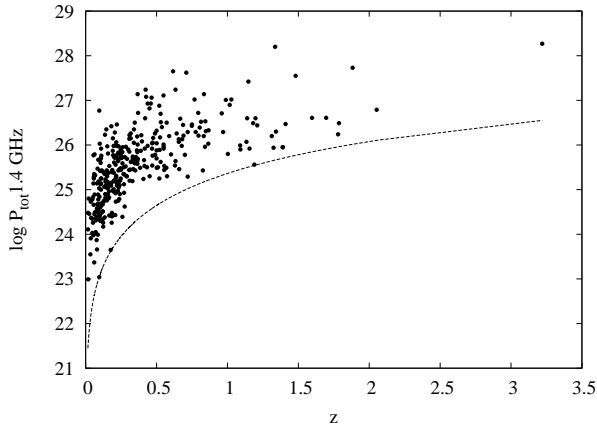


Figure 6. The total radio luminosity at 1.4 GHz as a function of redshift for a sample of GRSSs. The dashed line represents the total radio luminosity of the radio source with flux density of $S_{1.4GHz} = 5$ mJy, corresponding to the lowest flux density of sources in our catalogue.

tion of extragalactic radio sources have reported a decrease in median linear size with redshift for both bright and faint source samples (Neeser et al. 1995; Singal 1996) of the form $D \propto (1+z)^{-n}$, where n was found to have a range of values from about 1 to 3. These were consistent with the expectations of theoretical models (Kaiser & Alexander (1999)). However, such studies are complicated by possible correlations of size with luminosity, which may be different for galaxies and quasars (e.g. Singal 1988). Authors (e.g. Singal 1996) have stressed the importance of examining the D–z relationship for sources of similar radio luminosity, and perhaps separately for different classes. This would be possible for a large uniformly selected sample of giant sources, which is beyond the scope of the present paper. However, it may be relevant to note the recent paper by Onah et al. (2018) for a sample consisting of both galaxies and quasars, where

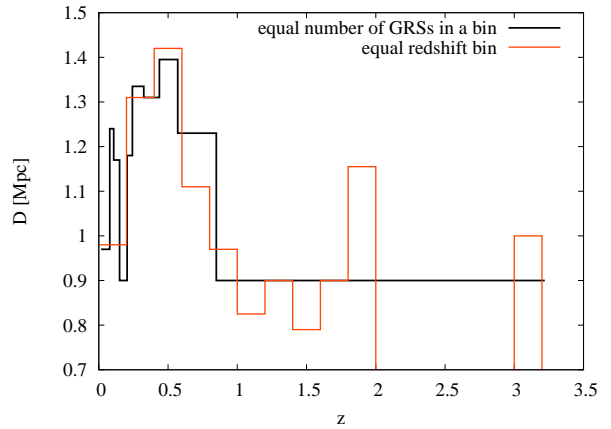


Figure 7. The GRSS's median size distribution as a function of redshift. Black line: the bins contain the same number of GRSSs – 35 sources each (except the last redshift bin which has 34 sources); red line: the bins are of equal redshift – bin size is equal to 0.2.

they report an increase in median size with redshift up to about $z=1$. In the context of GRSSs one also needs to examine whether large diffuse low-luminosity giants may be below the thresholds of existing surveys and observations.

The largest sample of GRSSs within the redshift range $1 < z < 2$ was presented by Kuligowska et al. (2009). Considering the dynamical evolution of radio galaxies, these authors concluded that the giant sizes of most distant objects are related rather to the very high power (up to 10^{40} W) of their jets, which overcomes the higher density of the IGM. These values are consistent with the location of these sources in the P–D diagram and the evolutionary models of radio sources.

4.5 GRSSs in regions of cosmic voids

Furthermore, to examine the dependence of GRSSs occurrence on the IGM density, we correlated the GRSS locations with the positions of 1228 cosmic voids provided by Mao, Berlind & Scherrer (2017). The catalogue of voids was compiled using the Baryon Oscillation Spectroscopic Survey (Dawson et al. 2013), which is a part of the SDSS-III (Eisenstein et al. 2011). The survey covers the sky area in a declination range of $-8^\circ < \delta < 66^\circ$ and contains voids with Galactic latitude $|b| > 20^\circ$ and in a redshift range of $0.2 < z < 0.67$. Within the sky area and redshift range covered by this void catalog, there are 91 GRGs of our compilation. However, we found just one clear correlation: the GRG J1355+2923 is located only about 17 Mpc from the centre (RA: $13^h 51^m 58^s.08$ Dec: $29^\circ 05' 34''$, J2000.0) of a void named ‘CMASS North 19434’ at $z=0.501$. The effective radius of the void is 40.5 Mpc. Although there have been a number of suggestions that GRGSs occur in regions of low IGM density (e.g. Machalski et al. 2006; Kuligowska et al. 2009, Chen et al. 2011, Malarecki et al. 2015), the above result suggests that the size of GRGSs is not related solely to the galaxy density around their host galaxies. Apart from deep X-ray observations, deeper optical observations including improved photometric redshifts (e.g. from PanSTARRS) could provide better estimates of the ambient galaxy density of GRGSs using the methods ap-

plied by [Komberg & Pashchenko \(2009\)](#), but out to higher redshifts.

5 CONCLUDING REMARKS

We present the largest-to-date sample of GRSs (defined here as having a projected largest linear size of at least 0.7 Mpc), which consists of 349 individual objects. It is limited by sensitivity and coverage of the available radio and optical surveys in different parts of the sky. Analysing the distribution of GRSs in the celestial plane, we distinguish sky regions that are underdense in GRSs and that should be explored for further objects yet to be identified even with current sensitivity limits. We estimate the lower limit to the number of GRSs on current sensitivity limits as ~ 2000 , based on the density of known GRSs in the regions where most such sources have been observed.

The present sample has considerably increased the number of GRSs with projected sizes larger than about 2 Mpc, and also at high redshifts of greater than ~ 1 . The Hubble diagram for the galaxies in the GRS sample has been found to be similar to that of 3CRR radio galaxies, with the *r*-band magnitude being well correlated with redshift, allowing for quick estimates of photometric redshifts for giants that have not been spectroscopically observed.

We have examined the luminosity–linear size diagram with the enlarged sample, and find the upper envelope to be well-defined for the GRSs. This is consistent with the evolution of the radio sources with the highest jet powers of $\sim 10^{40}$ W. The distribution is the result of different sources with different jet powers, as suggested by evolutionary scenarios (e.g. [Kaiser, Dennett-Thorpe & Alexander 1997](#); [Blundell, Rawlings & Willott 1999](#); [Ishwara-Chandra & Saikia 1999](#); [Machalski, Chyží & Jamrozy 2004](#)).

The high-redshift giants that are also amongst the more luminous ones can be understood in terms of their high jet powers ($\sim 10^{40}$ W), which overcomes the effects of higher ram pressure due to increased density of the IGM. This is consistent with the results of the P–D diagram.

While GRSs have been suggested to occur often in regions of low galaxy density, correlating our catalogue of GRSs with cosmic voids, we find only one clear association. Future X-ray telescopes will be useful for probing their environments from sensitive observations.

6 ACKNOWLEDGMENTS

We thank the reviewer Prof. H. Andernach for his very detailed and valuable comments that helped improve the paper significantly. A part of this project was supported by the Polish National Center of Science under decision UMO-2016/20/S/ST9/00142.

REFERENCES

- Albareti, F. D., Allende, P. C., Almeida, A., et al., 2017, *ApJS*, 233, 25
- Amirkhanyan, V. R., Afanasiev, V. L., & Moiseev, A. V., 2015, *AstBu*, 70, 45
- Andernach, H., Feretti, L., Giovannini, G., et al., 1992, *A&AS*, 93, 331
- Andernach, H., Jiménez Andrade, E. F., Maldonado Sánchez, R. F., & Vásquez Báez, I. R., 2012, Proceedings of the Science from the Next Generation Imaging and Spectroscopic Surveys Conference, 15–18 October 2012. Online at <http://www.eso.org/sci/meetings/2012/surveys2012/posters.html>, id. P1
- Bankowicz, M., Koziel-Wierzbowska, D., & Machalski, J., 2015, Proceedings of the SALT Science Conference (SSC2015), 1–5 June 2015. Stellenbosch Institute of Advanced Study. South Africa, Online at <http://pos.sissa.it/cgi-bin/reader/conf.cgi?confid=250>, id.34
- Bassani, L., Venturi, T., Molina, M., et al., 2016, *MNRAS*, 461, 3165
- Baum, S., A., & Heckman, T., 1989, *ApJ*, 336, 681
- Becker, R. H., White, R. L., & Helfand, D. J., 1995, *ApJ*, 450, 559
- Best, P. N., Kauffmann, G., Heckman, T. M., & Ivezić, Z., 2005, *MNRAS*, 362, 9
- Bhatnagar, S., Krishna, G., & Wisotzki, L., 1998, *MNRAS*, 299, 25
- Blundell, K. M., Rawlings, S., & Willott, C. J., 1999, *AJ*, 117, 677
- Bock, D. C.-J., Large, M. I., & Sadler, E. M., 1999, *AJ*, 117, 1578
- Brescia, M., Cavuoti, S., & Longo, G., 2015, *MNRAS*, 450, 3893
- Brown, M. J. I., Webster, R. L., & Boyle, B. J., 2001, *AJ*, 121, 2381
- Carilli, C. L., & Rawlings, S., 2004, *NewAR*, 48, 979
- Chen, R., Peng, B., Strom, R. G., & Wei, J., 2011, *MNRAS*, 412, 2433
- Clarke, A. O., Heald, G., Jarrett, T., et al., 2017, *A&A*, 601, 25
- Colafrancesco, S., Mhlahlo, N., Jarrett, T., Oozeer, N., & Marchegiani, P., 2016, *MNRAS*, 456, 512
- Condon, J. J., Cotton, W. D., Greisen, E. W., & Yin, Q. F., 1998, *AJ*, 115, 1693
- Cotter, G., Rawlings, S., & Saunders, R., 1996, *MNRAS*, 281, 1081
- Coziol, R., Andernach, H., Torres-Papaqui, J. P., Ortega-Minakata, R. A., & Moreno del Rio, F., 2017, *MNRAS*, 466, 921
- Dabhade, P., Gaikwad, M., Bagchi, J., et al., 2017, *MNRAS*, 469, 2886
- Dawson, K. S., Schlegel, D. J., Ahn, C. P., et al., 2013, *AJ*, 145, 10
- de Bruyn, A. G., 1989, *A&A*, 226, 13
- Djorgovski, S., Thompson, D. J., Vigotti, M., & Grueff, G., 1990, *PASP*, 102, 113
- Djorgovski, S. G., Thompson, D. J., Maxfield, L., Vigotti, M., & Grueff, G., 1995, *ApJS*, 101, 255
- Eales, S. A., 1985, *MNRAS*, 213, 899
- Eisenstein, D. J., Weinberg, D. H., Agol, E., et al., 2011, *AJ*, 142, 72
- Falco, E. E., Kurtz, M. J., Geller, M. J., et al., 1999, *PASP*, 111, 438
- Fananoff, B. L., & Riley, J. M., 1974, *MNRAS*, 167, 31
- Filipovic, M. D., Cajko, K. O., Collier, J. D., & Tothill, N. F. H., 2013, *SerAJ*, 187, 1
- Flewelling, H. A., Magnier, E. A., Chambers, K. C., et al., 2016, *2016arXiv161205243F*
- Fomalont, E. B., & Bridle, A. H., 1978, *AJ*, 83, 725
- Gehrels, N., Chincarini, G., Giommi, P., et al., 2004, *ApJ*, 611, 1005
- Gregg, M. D., Becker, R. H., & de Vries, W., 2006, *ApJ*, 641, 210
- Gupta, Y., Ajithkumar, B., Kale, H. S., et al., 2017, *Current Science*, 113, 707
- Hagen, H.-J., Engels, D., & Reimers, D., 1999, *A&AS*, 134, 483
- Hes, R., de Vries, W. H., & Barthel, P. D., 1995, *A&A*, 299, 17
- Hintzen, P., Ulvestad, J., & Owen, F., 1983, *AJ*, 88, 709

- Hota, A., Sirothia, S. K., Ohyama, Y., et al., 2011, MNRAS, 417L, 36
- Högblom, J. A., 1979, A&AS, 36, 173
- Hunik, D., & Jamrozy, M., 2016, ApJ, 817, 1
- Hurley-Walker, N., Johnston-Hollitt, M., Ekers, R., et al., 2015, MNRAS, 447, 2468
- Ishwara-Chandra, C. H., & Saikia, D. J., 1999, MNRAS, 309, 100
- Jägers, W.J., 1986, PhD thesis, University of Leiden
- Jamrozy, M., Konar, C., Machalski, J., & Saikia, D. J., 2008, MNRAS, 385, 1286
- Jones, P. A., & McAdam, W. B., 1992, ApJS, 80, 137
- Jones, D. H., Read, M. A., Saunders, W., et al., 2009, MNRAS, 399, 683
- Kapahi, V.K. 1989, AJ, 97, 1
- Kapahi, V. K., Athreya, R. M., van Breugel, W., McCarthy, P.J., & Subrahmanya, C.R., 1998, ApJS, 118, 275
- Kaiser, C. R., & Alexander, P., 1999, MNRAS, 302, 515
- Kaiser, C. R., Dennett-Thorpe, J., & Alexander, P., 1997, MNRAS, 292, 723
- Kharb, P., O'Dea, C. P., & Baum, S. A., 2008, ApJS, 174, 74
- Klein, U., Mack, K.-H., Gregorini, L., & Vigotti, M., 2003, A&A, 406, 579
- Konar, C., Saikia, D. J., Ishwara-Chandra, C. H., & Kulkarni, V. K., 2004, MNRAS, 355, 845
- Konar, C., Saikia, D. J., Jamrozy, M., & Machalski, J., 2006, MNRAS, 372, 693
- Koziel-Wierzbowska, D., & Stasińska, G., 2011, MNRAS, 415, 1013
- Kronberg, P. P., Wielebinski, R., & Graham, D. A., 1986, A&A, 169, 63
- Komberg, B. V., & Pashchenko, I. N., 2009, ARep, 53, 1086
- Kuligowska, E., Jamrozy, M., Koziel-Wierzbowska, D., & Machalski, J., 2009, AcA, 59, 431
- Kuźmicz, A., Kuligowska, E., & Jamrozy, M., 2011, AcA, 61, 71
- Kuźmicz, A., & Jamrozy, M., 2012, MNRAS, 426, 851
- Lacy, M., Rawlings, S., & Warner, P. J., 1992, MNRAS, 256, 404
- Lacy, M., Rawlings, S., Saunders, R., & Warner P. J., 1993, MNRAS, 264, 721
- Lacy, M., Rawlings, S., Hill, G. J., et al., 1999, MNRAS, 308, 1096
- Lacy, M., 2000, ApJ, 536, 1
- Laing, R. A., Riley, J. M., & Longair, M. S., 1983, MNRAS, 204, 151
- Lara, L., Márquez, I., Cotton, W. D., et al., 1999, A&A, 348, 699
- Lara, L., Mack, K. H., Lacy, M., et al., 2000, A&A, 356, 63
- Lara, L., Cotton, W. D., Feretti, L., et al., 2001a, A&A, 370, 409
- Lara, L., Marquez, I., Cotton, W. D., et al., 2001b, A&A, 378, 826
- Law-Green, J. D. B., Eales, S. A., Leahy, J. P., Rawlings, S., & Lacy, M., 1995, MNRAS, 277, 995
- Leahy, J. P., & Perley, R. A., 1991, AJ, 102, 537
- Lonsdale, C. J., Cappallo, R. J., Morales, M. F., et al., 2009, IEEEIP, 97, 1497
- Machalski, J., 1998a, A&AS, 128, 153
- Machalski, J., & Condon, J. J., 1999, APJS, 123, 41
- Machalski, J., Chyžý, K. T., & Jamrozy, M., 2004, AcA, 54, 391
- Machalski, J., Jamrozy, M., & Saikia, D. J., 2009, MNRAS, 395, 812
- Machalski, J., Jamrozy, M., & Zoła, S., 2001, A&A, 371, 445
- Machalski, J., Jamrozy, M., Zoła, S., & Kozięć, D., 2006, A&A, 454, 85
- Machalski, J., Koziel-Wierzbowska, D., & Jamrozy, M., 2007, AcA, 57, 227
- Machalski, J., Koziel-Wierzbowska, D., Jamrozy, M., & Saikia, D. J., 2008, ApJ, 679, 149
- Machalski, J., Jamrozy, M., Stawarz, L., & Koziel-Wierzbowska, D., 2011, ApJ, 740, 58
- Mack, K. H., Klein, U., O'Dea, C. P., & Willis, A. G., 1997, A&AS, 123, 423
- Mack, K.-H., Klein, U., O'Dea, C. P., Willis, A. G., & Saripalli, L., 1998, A&A, 329, 431
- Mack, K. H., Vigotti, M., Gregorini, L., et al., 2005, A&A, 435, 863
- Malarecki, J. M., Jones, D. H., Saripalli, L., Staveley-Smith, L., & Subrahmanyan, R., 2015, MNRAS, 449, 955
- Malarecki, J. M., Staveley-Smith, L., Saripalli, L., et al., 2013, MNRAS, 432, 200
- Malkin, Z., 2016, “A new method to subdivide a spherical surface into equal-area cells”, arXiv:1612.03467
- Mao, Q., Berlind, A. A., & Scherrer, R. J., 2017, ApJ, 835, 161
- Marecki, A., Jamrozy, M., & Machalski, J., 2016, MNRAS, 463, 338
- Masetti, N., Parisi, P., & Palazzi, E., 2013, A&A, 556, 120
- McCarthy, P. J., Miley, G. K., de Koff, S., et al., 1997, ApJS, 112, 415
- Molina, M., Bassani, L., Malizia, A., et al., 2014, A&A, 565, 2
- Molina, M., Venturi, T., Malizia, A., et al., 2015, MNRAS, 451, 2370
- Murgia, M., Fanti, C., Fanti, R., et al., 1999, A&A, 345, 769
- Murgia, M., 2003, Publ. Astron. Soc. Aust., 20, 19
- Murgia, M., Parma, P., Mack, K.-H., et al., 2011, A&A, 526, 148
- Neeser, M. J., Eales, S. A., Law-Green, J. D., Leahy, J. P., & Rawlings, S., 1995, ApJ, 451, 76
- Nilsson, K., 1998, A&AS, 132, 31
- Onah, C. I., Ubachukwu, A. A., Odo, F. C., & Onuchukwu, C. C., 2018, RMxAA, 54, 271
- Owen, F. N., Ledlow, M. J., Eilek, J. A., et al., 2002, IAUS, 199, 171
- Parma, P., de Ruiter, H. R., Mack, K. H., et al., 1996, A&A, 311, 49
- Parma, P., Murgia, M., & Morganti, R., 1999, A&A, 344, 7
- Peng, B., Chen, R.-R., & Strom, R., 2015, “Giant radio galaxies as probes of the ambient WHIM in the era of the SKA” in proc. Advancing Astrophysics with the Square Kilometre Array, PoS(AASKA14)109, arXiv:1501.00407
- Piryá, A., Saikia, D. J., Singh, M., & Chandola, H. C., 2012, MNRAS, 426, 758
- Proctor, D. D., 2011, ApJS, 194, 31
- Proctor, D. D., 2016, ApJS, 224, 18
- Reid, R. I., Kronberg, P. P., & Perley, R. A., 1999, ApJS, 124, 285
- Rengelink, R. B., Tang, Y., de Bruyn, A. G., et al., 1997, A&AS, 124, 259
- Rentería Macario, J., & Andernach, H., 2017, arXiv:171010731R
- Riley, J. M. A., Warner, P. J., Rawlings, S., et al., 1989, MNRAS, 236, 13
- Röttgering, H. J. A., Tang, Y., Bremer, M. A. R., et al., 1996, MNRAS, 282, 1033
- Sadler, E. M., Jackson, C. A., Cannon, R. D., et al., 2002, MNRAS, 329, 227
- Sadler, E. M., Cannon, R. D., & Mauch, T., 2007, MNRAS, 381, 211
- Saikia, D. J., & Jamrozy, M., 2009, BASI, 37, 63
- Saikia, D. J., Konar, C., & Kulkarni, V. K., 2006, MNRAS, 366, 139
- Santiago-Bautista, I., Rodriguez-Rico, C. A., Andernach, H., et al., 2016, in The Universe of Digital Sky Surveys, Vol. 42, ed. Napolitano N.R., Longo G., Marconi M., Paolillo M., Iodice E., ASSP, 42, 231
- Saripalli, L., Gopal-Krishna, R. W., & Kuehr, H., 1986, A&A, 170, 20
- Saripalli, L., Subrahmanyan, R., & Hunstead, R. W., 1994, MNRAS, 269, 37
- Saripalli, L., Patnaik, A. R., Porcas, R. W., & Graham, D. A., 1997, A&A, 328, 78

- Saripalli, L., Hunstead, R. W., Subrahmanyam, R., & Boyce, E., 2005, AJ, 130, 896
- Saripalli, L., Subrahmanyam, R., Laskar, T., & Koekemoer, A., 2008, in *From Planets to Dark Energy: The Modern Radio Universe*, Proceedings of Science, 130 (astro-ph: 0806.3518)
- Saripalli, L., Subrahmanyam, R., Thorat, K., et al., 2012, ApJS, 199, 27
- Saunders, R., Baldwin, J. E., & Warmer, P. J., 1987, MNRAS, 225, 713
- Schoenmakers, A. P., Mack, K. H., Lara, L., et al., 1998, A&A, 336, 455
- Schoenmakers, A. P., de Bruyn, A. G., Röttgering, H. J. A., van der Laan, H., & Kaiser, C. R., 2000a, MNRAS, 315, 371
- Schoenmakers, A. P., Mack, K. H., de Bruyn, A. G., et al., 2000b, A&AS, 146, 293
- Schoenmakers, A. P., de Bruyn, A. G., Röttgering, H. J. A., & van der Laan, H., 2001, A&A, 374, 861
- Sebastian, B., Ishwara-Chandra, C. H., Joshi, R., & Wadadekar, Y., 2018, MNRAS, 473, 4926
- Simpson, C., Martinez-Sansigre, A., Rawlings, S., et al., 2006, MNRAS, 372, 741
- Singal, A. K., 1988, MNRAS, 233, 87
- Singal, A. K., 1996, IAUS, 175, 563
- Singal, A. K., Konar, C., & Saikia, D. J., 2004, MNRAS, 347, 79
- Skrutskie, M.F., Cutri, R.M., Stiening, R., et al. 2006, AJ, 131, 1163
- Solovyov, D. I., & Verkhodanov, O. V., 2014, AstBu, 69, 141
- Subrahmanyam, R., Saripalli, L., & Hunstead, R. W., 1996, MNRAS, 279, 257
- Subrahmanyam, R., Saripalli, L., Safouris, V., & Hunstead, R. W., 2008, ApJ, 677, 63
- Subrahmanyam, R., Ekers, R. D., Saripalli, L., & Sadler, E. M., 2010, MNRAS, 402, 2792
- Tamhane, P., Wadadekar, Y., Basu, A., et al., 2015, MNRAS, 453, 2438
- van Breugel W. J. M., & Willis A. G., 1981, A&A, 96, 332
- van Breugel, W. J. M., & Jägers, W., 1982, A&AS, 49, 529
- van Haarlem, M. P., Wise, M. W., Gunst, A. W., et al. 2013, A&A, 556, 2
- Weźgowiec, M., Jamrozy, M., & Mack, K.-H., 2016, AcA, 66, 85
- Willis, A. G., Strom, R. G., & Wilson, A. S., 1974, Nature, 250, 625
- Wing, J. D., & Blanton, E. L., 2011, AJ, 141, 88
- Winkler, C., 1994, ApJS, 92, 327
- Wright, E. L., Eisenhardt, P. R. M., Mainzer, A. K., et al., 2010, AJ, 140, 1868

Table 1: List of GRSs

IAU name (1)	α (2000) (h m s) (2)	δ (2000) ($^{\circ}$ $'$ $''$) (3)	ID (4)	z (5)	FR type (6)	LAS (arcmin) (7)	D (Mpc) (8)	r (mag) (9)	S_I (mJy) (10)	δS_I (mJy) (11)	$\log P_{tot}$ W/Hz (12)	Ref. (13)
J0003+0351	00 03 31.50	+03 51 11.3	G	0.0953	II	19.5	2.03	17.048	484.8	24.7	25.03	1
J0003−1517	00 03 49.08	−15 17 33.9	G	0.1051	II	8.3	0.95	16.751	480.8	14.4	25.12	2
J0010−1108	00 10 49.69	−11 08 13.0	G	0.0773	II	9.2	0.80	16.296	52.9	1.6	23.87	3
J0016+0420	00 16 04.36	+04 20 24.2	G	0.4328	II	6.9	2.40	19.726	50.0	5.0	25.50	4
J0017−2223	00 17 47.79	−22 23 19.8	G	0.1081	II	9.8	1.14	16.868	479.8	24.2	25.14	5
J0020−2016	00 20 33.28	−20 16 10.0	G	0.1970	II	6.2	1.20	18.488	907.2	27.3	25.98	6
J0022−0818	00 22 24.96	−08 18 45.7	G	0.5715	II	6.2	2.50	20.547	259.0	24.0	26.50	4,1
J0023−6710	00 23 40.33	−67 10 54.9	G	(1.41)	II	1.4	0.71	22.67r	28.1 ^a		26.47	7
J0028−6631	00 28 57.83	−66 31 14.9	G	(1.78)	II	1.8	0.90	23.26r	9.6 ^a		26.24	7
J0031−6727	00 31 48.01	−67 27 19.9	G	1.1560	II	1.7	0.85	19.24r	12.7 ^a		25.92	7
J0034−6639	00 34 05.63	−66 39 35.0	G	0.1075	II	16.5	1.93	16.79r	101.9 ^b	6.3	24.47	8
J0037+0027	00 37 54.59	+00 27 17.4	G	0.5893	II	5.3	2.11	20.805	122.1	3.7	26.20	9
J0039−1300	00 39 39.88	−13 00 59.8	G	0.1075	II	10.7	1.23	16.856	153.1	4.6	24.63	3
J0041+3225	00 41 46.62	+32 25 09.6	G	(0.45)	II	2.8	0.97	19.119	959.4	28.8	26.82	10
J0042−0613	00 42 46.85	−06 13 52.9	G	0.1243	II	6.5	0.85	17.484	637.5	19.1	25.39	3
J0044−6656	00 44 46.94	−66 56 40.0	G	(0.72)	II	1.8	0.78	21.01r	9.3 ^a		25.29	7
J0047+5339	00 47 16.65	+53 39 36.8	G	0.1460	II	16.0	2.43	17.803	114.6	3.4	24.80	11
J0047−8308	00 47 55.50	−83 08 12.5	G	0.2591	II	5.6	1.34		533.0 ^c	16.0	25.84	12
J0051−2028	00 51 07.10	−20 28 25.1	G	0.0856	II	8.0	0.76	16.718	186.6	9.8	24.52	5
J0053+4031	00 53 31.69	+40 31 25.8	G	0.1488	II	7.6	1.17	18.018	468.0	14.2	25.43	13
J0057−6606	00 57 26.75	−66 06 33.5	G	(1.39)	II	1.5	0.76	22.65r	8.9 ^a		25.95	7
J0057+3021	00 57 48.88	+30 21 08.8	G	0.0165	I/II	58.0	1.13		2320	69.8	24.11	14
J0104−6609	01 04 21.97	−66 09 26.7	G	(1.19)	II	1.5	0.75	22.26r	5.2 ^a		25.56	7
J0104−6704	01 04 31.78	−67 04 37.9	G	(1.39)	II	1.5	0.76	22.64r	8.8 ^a		25.95	7
J0106−6645	01 06 47.72	−66 45 51.2	G	(1.21)	II	1.8	0.90	22.29r	38.3 ^a		26.44	7
J0107+3224	01 07 24.96	+32 24 45.2	G	0.0170	I	40.0	0.82	14.578	4746	142.4	24.48	15
J0109+7311	01 09 43.60	+73 11 56.0	G	0.1810	II	4.0	0.72	20.205	3018	90.5	26.42	16
J0112+4928	01 12 02.24	+49 28 35.0	G	0.0670	II	10.6	0.81	16.875	1977	59.4	25.32	17
J0115+2507	01 15 57.23	+25 07 21.0	G	0.1836	II	5.8	1.06	17.925	157.4	4.7	25.16	2
J0116−4722	01 16 25.05	−47 22 41.6	G	0.1461	II	11.7	1.78		4077 ^b	122.9	26.35	18
J0117−0111	01 17 34.84	−01 11 35.6	Q	0.1855	II	5.2	0.96	19.504	33.0	2.6	24.48	1
J0117+0026	01 17 46.30	+00 26 22.1	G	0.5540	II	3.7	1.42	20.651	24.3	1.9	25.44	1
J0120−0038	01 20 12.51	−00 38 37.6	G	0.2354	I	3.2	0.71	18.515	310.6	9.4	25.69	19
J0129−0758	01 29 35.26	−07 58 04.3	G	0.0991	I/II	12.0	1.30	16.441	107.1	3.2	24.41	3
J0133−1303	01 33 13.53	−13 03 30.5	G	(0.289)	II	6.9	1.79	18.940	80.4	2.4	25.30	20
J0134−0107	01 34 12.78	−01 07 29.5	G	0.0790	I/II	13.7	1.21	16.226	258.8	7.8	24.58	3
J0135−0044	01 35 25.66	−00 44 47.3	G	0.1564	II	6.6	1.06	17.884	195.9	5.9	25.09	2

Table 1 continued

IAU name (1)	α (2000) (h m s) (2)	δ (2000) (° ' '') (3)	ID (4)	z (5)	FR type (6)	LAS arcmin (7)	D (Mpc) (8)	r (mag) (9)	S_I (mJy) (10)	δS_I (mJy) (11)	$\log P_{tot}$ W/Hz (12)	Ref. (13)
J0135+3754	01 35 28.33	+37 54 05.6	G	0.4373	II	2.7	0.91	19.422	1331	40.0	26.93	21
J0139+3957	01 39 30.46	+39 57 03.3	G	0.2107	II	5.7	1.17	18.735	794.5	23.9	25.99	22
J0143-5431	01 43 43.13	-54 31 39.3	G	0.1791	II	5.5	0.99		217.0 ^c	6.5	25.09	12
J0152+0015	01 52 14.26	+00 15 02.6	G	0.8440	II	2.2	1.03	20.818	111.6	3.4	26.53	23
J0155-2654	01 55 46.30	-26 54 04.7	G	0.2091	II	3.8	0.77	17.843	22.3	0.7	24.43	24
J0157+0209	01 57 52.52	+02 09 54.0	G	0.2217	II	7.0	1.49	18.572	691.3	20.7	25.98	11
J0200+4048	02 00 30.10	+40 48 53.1	G	0.0827	I/II	14.0	1.30		283.5	9.0	24.67	13
J0202-0939	02 02 24.09	-09 39 00.3	G	0.7683	II	2.6	1.12	20.948	433.7	21.7	27.02	1,3
J0204-0944	02 04 48.29	-09 44 09.5	Q	1.0033	II	4.2	2.08	18.904	13.6	0.4	25.80	25
J0210+0118	02 10 08.48	+01 18 39.6	Q	0.8652	II	2.6	1.21	18.595	33.1	1.0	26.03	25
J0213-4744	02 13 09.53	-47 44 13.4	G	0.2200	II	6.3	1.33		2115 ^b	64.3	26.46	18
J0214+3251	02 14 15.38	+32 51 05.3	G	0.2610	II	5.2	1.25	19.068	451.1	13.6	25.95	26
J0216-0449	02 16 59.24	-04 49 20.3	G	1.3250	II	2.4	1.20		9.6	0.3	25.94	27,28
J0237-6430	02 37 10.07	-64 30 01.5	G	0.3640	II	6.6	2.00		154.0 ^c	4.6	25.64	12
J0241+0038	02 41 39.69	+00 38 31.7	G	0.6341	II	3.8	1.56	20.957	27.9	1.9	25.64	1
J0259+0018	02 59 42.88	+00 18 40.9	G	0.1834	II	4.0	0.73	17.918	20.3	2.0	24.26	29
J0300-0728	03 00 59.06	-07 28 30.8	G	0.4905	II	5.0	1.81	20.611	71.9	2.2	25.78	3
J0313+4120	03 13 01.96	+41 20 01.2	G	0.1340	I/II	9.5	1.34	17.359	489.8	14.8	25.35	30
J0313-0631	03 13 32.88	-06 31 57.9	Q	0.3889	II	3.5	1.11	19.325	151.8	4.6	25.87	3
J0315-0743	03 15 36.19	-07 43 38.8	G	(0.269)	II	3.3	0.86	19.140	151.0	16.0	25.50	4
J0316-2658	03 16 04.24	-26 58 06.0	G	0.2171	II	3.8	0.79	17.466	453.5	13.8	25.77	6
J0318+6829	03 18 18.98	+68 29 31.4	G	0.0901	II	14.9	1.48	18.650	777.5	23.5	25.18	31
J0320-4515	03 20 57.54	-45 15 10.7	G	0.0630	II	25.6	1.84		6657 ^b	201.7	25.79	32
J0326-7730	03 26 01.33	-77 30 16.0	G	0.2771	II	5.3	1.33		357.0 ^c	10.7	25.73	12
J0331-7713	03 31 39.79	-77 13 19.2	G	0.1456	II	17.7	2.69		687.0 ^c	20.6	25.40	12
J0349+7511	03 49 16.28	+75 11 22.0	G	0.0803	II	14.5	1.30	16.609	30	0.9	23.66	33
J0351-1429	03 51 28.54	-14 29 08.7	Q	0.6163	II	2.1	0.84	15.890	3049	91.5	27.65	34
J0401-8456	04 01 18.32	-84 56 36.1	G	0.1037	I	6.3	0.71		175.0 ^c	5.3	24.49	12
J0408-6247	04 08 46.07	-62 47 51.3	G	0.0178	II	33.0	0.71		210.0 ^b	20.0	22.99	35
J0422+1510	04 22 20.85	+15 10 59.5	G	0.0720	I	13.6	1.10	18.123	168.8	24.31	36	
J0423-7246	04 23 57.57	-72 46 01.6	G	0.1921	II	4.1	0.78		2143 ^b	65.3	26.15	18
J0429+0033	04 29 25.85	+00 33 04.8	Q	(0.468)	II	5.4	1.90	19.945	111.0	10.0	25.92	4
J0430+7722	04 30 49.49	+77 22 58.4	G	0.2150	II	4.9	1.02	19.189	143.8	4.6	25.27	37
J0439-2422	04 39 09.20	-24 22 08.0	Q	0.8340	II	2.1	0.96	17.782	454.6	13.7	27.14	38
J0443-6141	04 43 44.69	-61 41 40.2	Q	0.7200	II	1.7	0.73		93.3 ^a		26.29	39
J0449+4500	04 49 09.08	+45 00 39.2	G	0.0208	I	30.0	0.76	17.858	6502	195.1	24.80	40
J0449-3026	04 49 32.35	-30 26 37.7	Q	0.3149	II	7.5	2.14	17.945	94.0	9.0	25.45	4

Table 1 continued

IAU name (1)	α (2000) (h m s) (2)	δ (2000) (° ' '') (3)	ID (4)	z (5)	FR type (6)	LAS (arcmin) (7)	D (Mpc) (8)	r (mag) (9)	S_I (mJy) (10)	δS_I (mJy) (11)	$\log P_{tot}$ W/Hz (12)	Ref. (13)
J0452+5204	04 52 52.84	+52 04 47.1	G	0.1090	I	9.7	1.15	17.530	2853	85.6	25.92	40
J0459–5250	04 59 16.33	–52 50 08.1	G	0.0959	II	9	0.90		7.3 ^b	1.0	23.04	41
J0505–2835	05 05 49.22	–28 35 19.4	G	0.0381	II	40.0	1.79		713.9	21.8	24.37	42
J0508+6056	05 08 27.26	+60 56 27.3	G	0.0710	I	10.4	0.84	17.638	189.7	6.1	24.35	37
J0513–3028	05 13 31.98	–30 28 50.1	G	0.0576	II	11.4	0.76	15.987	2279	68.4	25.25	18
J0515–8059	05 15 55.18	–80 59 43.1	G	0.1049	I/II	7.5	0.86		267.0 ^c	8.0	24.68	12
J0547+0108	05 47 13.74	+01 08 50.4	G	(0.135) ^p	II	7.1	1.01	19.515	199.4	6.0	25.07	2
J0607+6114	06 07 34.92	+61 14 43.5	G	0.2270	I/II	5.3	1.15	18.895	346.4	10.6	25.70	37
J0632–5404	06 32 01.17	–54 04 57.5	Q	0.2036	II	5.2	1.04		694.0 ^c	20.8	25.72	12
J0636–2034	06 36 32.26	–20 34 53.2	G	0.0552	II	15.0	0.95	16.267	8485	254.6	25.77	43
J0652+4304	06 52 18.38	+43 04 59.7	G	0.0891	II	9.6	0.95	16.678	315.7	9.8	24.78	26
J0654+7319	06 54 26.69	+73 19 50.2	G	0.1145	II	12.6	1.56	18.644	828.6	24.9	25.43	26
J0657+4808	06 57 51.78	+48 08 29.7	G	0.7760	II	2.2	0.98	20.697	78.2	2.6	26.29	44
J0702+4859	07 02 06.24	+48 59 20.1	G	0.0649	I/II	19.1	1.41	15.848	316.2	9.8	24.49	26
J0709–3601	07 09 14.09	–36 01 21.8	G	0.1108	II	8.2	0.98		1902	57.1	25.76	18
J0720+2837	07 20 14.37	+28 37 23.3	G	0.2710	II	6.3	1.56	18.477	39.9	1.8	24.93	45
J0725+3025	07 25 17.39	+30 25 36.3	G	(0.70)	II	2.9	1.24	19.745	31.0	1.5	25.78	46
J0745+0200	07 45 04.47	+02 00 08.1	G	0.4650	II	2.1	0.74	20.220	1535	46.0	27.06	47
J0746–5702	07 46 18.62	–57 02 58.2	G	0.1300	I	7.4	1.02		194.0 ^c	5.8	24.74	12
J0748+5548	07 48 36.87	+55 48 58.3	G	0.0356	II	34.0	1.44	15.806	1822	54.7	24.73	14
J0750+6541	07 50 34.40	+65 41 25.6	Q	0.7490	II	3.7	1.63	17.702	116.7	3.8	26.43	37
J0751+4231	07 51 08.80	+42 31 24.2	G	0.2042	II	6.0	1.19	18.142	138.3	4.5	25.19	26
J0754+4316	07 54 07.96	+43 16 10.6	Q	0.3476	II	8.1	2.37	16.722	101.9	3.5	25.59	25,26
J0754+3033	07 54 48.85	+30 33 55.0	Q	0.7961	II	3.8	1.71	17.727	60.7	1.8	26.21	25
J0801+4736	08 01 31.97	+47 36 16.1	Q	0.1567	II	6.0	0.97	15.642	124.9	4.0	24.90	25,26
J0802+4927	08 02 48.80	+49 27 23.8	G	(0.678)	II	4.3	1.88	21.317	52.0	7.0	25.98	4
J0803+6656	08 03 45.83	+66 56 11.4	G	0.2470	II	4.7	1.08	20.629	174.0	5.5	25.48	37
J0807+7400	08 07 10.16	+74 00 41.8	G	0.1204	II	9.1	1.17	17.175	128.8	4.4	24.67	26
J0809+2912	08 09 06.22	+29 12 35.6	Q	1.4807	II	2.2	1.10	17.582	300.6	9.0	27.55	48
J0810–6800	08 10 55.10	–68 00 07.7	Q	0.2311	II	6.5	1.43		271.0 ^c	8.1	25.43	12
J0812+3031	08 12 40.08	+30 31 09.4	Q	1.3127	II	2.4	1.23	18.533	18.1	0.5	26.20	48
J0813+4516	08 13 10.80	+45 16 01.4	G	0.2204	II	6.9	1.46	18.877	107.7	3.7	25.16	26
J0816+3347	08 16 35.52	+33 47 48.6	Q	0.5099	II	3.5	1.29	19.669	34.4	1.6	25.50	46
J0819+0549	08 19 41.12	+05 49 42.6	Q	1.6959	II	1.9	0.99	20.531	24.8	0.7	26.61	48
J0819+7538	08 19 50.50	+75 38 39.5	G	0.2324	II	8.3	1.83	18.487	607.8	18.4	25.97	26
J0824+0140	08 24 18.16	+01 40 40.2	G	0.2125	II	4.8	0.99	17.936	43.4	1.3	24.73	3
J0826+6920	08 26 01.01	+69 20 37.0	G	0.5380	II	6.7	2.54	21.133	238.8	4.6	26.40	49
J0842+2147	08 42 39.95	+21 47 10.3	Q	1.1814	II	2.2	1.08	18.948	44.9	1.3	26.49	48

Table 1 continued

IAU name (1)	α (2000) (h m s) (2)	δ (2000) (° ' '') (3)	ID (4)	z (5)	FR type (6)	LAS arcmin (7)	D (Mpc) (8)	r (mag) (9)	S_I (mJy) (10)	δS_I (mJy) (11)	$\log P_{tot}$ W/Hz (12)	Ref. (13)
J0843-7006	08 43 05.41	-70 06 56.1	G	0.1393	I	6.9	1.01	17.651	203.0 ^c	6.1	24.82	12
J0843+2037	08 43 47.84	+20 37 52.4	Q	0.2276	II	5.4	1.17		62.0	1.9	24.96	50
J0844+4627	08 44 08.85	+46 27 44.2	G	0.5697	II	5.5	2.14	20.816	82.3 ^d	2.5	25.49	51
J0856+6621	08 56 16.32	+66 21 26.8	G	0.4890	II	3.8	1.37	20.289	216.4	6.6	26.26	37
J0857+0131	08 57 01.76	+01 31 30.9	G	0.2734	II	5.2	1.30	18.953	99.0	9.0	25.34	4
J0857+3945	08 57 43.54	+39 45 28.7	G	0.5288	II	2.8	1.05	19.962	501.8	15.1	26.70	21
J0858+5620	08 58 32.78	+56 20 15.0	G	0.2402	II	3.9	0.88	19.035	77.4	2.3	25.10	2
J0902+5707	09 02 07.20	+57 07 37.9	Q	1.5964	II	1.7	0.87	18.749	29.3	0.9	26.61	52
J0902+1737	09 02 38.42	+17 37 51.5	G	0.1645	II	7.1	1.19	17.749	129.5	3.9	24.96	2
J0903+1208	09 03 03.53	+12 08 58.6	G	0.3444	II	5.3	1.54	19.267	107.9	3.2	25.60	3
J0908+3942	09 08 18.57	+39 42 57.1	G	1.8830	II	1.9	0.97	21.098	259.2	7.9	27.73	53
J0908+3506	09 08 47.89	+35 06 21.9	G	0.2600	II	6.3	1.51	18.483	196.6	6.1	25.59	26
J0912+3510	09 12 51.67	+35 10 12.0	G	0.2489	II	6.3	1.46	19.374	153.2	2.9	25.44	45
J0914+1006	09 14 19.52	+10 06 40.6	G	0.3080	II	6.3	1.71	18.729	483.3	14.5	26.14	2
J0918+2325	09 18 58.15	+23 25 55.4	Q	0.6899	II	2.1	0.89	17.818	85.9	2.6	26.21	25
J0918+3151	09 18 59.41	+31 51 40.7	G	0.0621	I	11.0	0.78	15.885	314.5	9.7	24.45	40
J0922+0919	09 22 21.60	+09 19 05.2	G	(0.23)	II	7.2	1.57	18.909	98.2	4.9	25.17	3
J0925-0114	09 25 12.73	-01 14 41.3	G	0.0730	II	13.9	1.14	16.344	82.5	2.5	24.02	3
J0925+4004	09 25 54.72	+40 04 14.2	Q	0.4717	II	4.4	1.55	17.891	75.5	2.3	25.76	25
J0926+6519	09 26 00.82	+65 19 22.7	G	0.1397	I	5.3	0.78	17.125	300.9	9.2	25.18	37
J0926+6100	09 26 53.38	+61 00 25.2	Q	0.2430	II	3.7	0.84	18.758	93.2	3.3	25.20	37
J0927+3511	09 27 49.38	+35 11 04.2	G	(0.55)	II	5.8	2.23	17.455	83.4	2.9	25.96	46
J0929+4146	09 29 10.67	+41 46 45.5	G	0.3650	II	6.6	2.00	19.792	164.6	5.4	25.84	26
J0931+3204	09 31 39.05	+32 04 00.1	Q	0.2267	II	19.9	4.29	17.487	65.6	2.0	24.97	50
J0932+1611	09 32 38.30	+16 11 57.2	G	0.1910	II	4.0	0.76	17.817	746.3	22.5	25.87	54
J0937+2937	09 37 04.04	+29 37 04.8	Q	0.4513	II	2.6	0.90	17.699	28.9	0.9	25.30	25
J0939+7405	09 39 47.07	+74 05 29.8	G	0.1215	II	7.3	0.95	16.765	87.6	3.3	24.51	26
J0939+3553	09 39 52.76	+35 53 58.9	G	0.1367	II	5.4	0.78	17.444	3542	106.3	26.23	55
J0944+2331	09 44 18.84	+23 31 19.8	Q	0.9890	II	1.9	0.91	17.914	229.1	6.9	27.01	25
J0947-1338	09 47 08.00	-13 38 27.7	G	0.0800	II	25.2	2.26	16.711	915.9	27.5	25.14	3
J0949+7314 ⁿ	09 49 45.86	+73 14 23.1	G	0.0581	II	14.7	0.98	16.173	2522	75.8	25.29	37
J0952+2352	09 52 06.38	+23 52 45.2	Q	0.9696	II	1.5	0.70	17.440	45.1	1.5	26.29	25
J0954+2715	09 54 19.19	+27 15 59.9	G	0.4712	II	3.9	1.37	19.895	146.4	4.4	26.05	2
J0959+1216	09 59 34.49	+12 16 31.5	Q	1.0895	II	2.0	0.98	18.686	17.1	0.5	25.99	25
J1004+5434	10 04 51.83	+54 34 04.4	G	0.0471	II	14.9	0.81	15.587	214.0	6.4	24.03	26
J1005-1315	10 05 57.45	-13 15 24.1	G	(0.31)	II	4.3	1.17	19.579	53.9	1.6	25.20	3
J1006+3454	10 06 01.74	+34 54 10.4	G	0.0994	II	39.0	4.23	16.759	4481	134.5	26.03	21
J1011+3111	10 11 12.11	+31 11 04.5	G	(0.50)	II	4.8	1.75	21.556	57.3	2.1	25.70	46

Table 1 continued

IAU name (1)	α (2000) (h m s) (2)	δ (2000) (° ' '') (3)	ID (4)	z (5)	FR type (6)	LAS arcmin (7)	D (Mpc) (8)	r (mag) (9)	S_I (mJy) (10)	δS_I (mJy) (11)	$\log P_{tot}$ W/Hz (12)	Ref. (13)
J1012+4229	10 12 44.29	+42 29 57.0	G	0.3651	II	3.1	0.94	17.906	89.4	2.7	25.58	25
J1014–0146	10 14 43.93	−01 46 11.9	G	0.1986	II	4.9	0.96	17.840	224.2	6.7	25.38	3
J1018–1240	10 18 49.83	−12 40 55.1	G	0.0793	I/II	9.3	0.81	17.163	226.3	6.8	24.51	56
J1020+0447	10 20 26.86	+04 47 52.0	Q	1.1338	II	1.5	0.74	19.191	19.0	0.6	26.07	25
J1020+3958	10 20 41.15	+39 58 11.2	Q	0.8266	II	2.7	1.23	18.092	9.2	0.3	25.43	25
J1021–0236	10 21 03.08	−02 36 42.6	G	0.2920	II	6.0	1.56	19.029	193.4	5.8	25.69	3
J1021+1217	10 21 24.22	+12 17 05.5	G	0.1294	II	14.4	1.97	17.301	134.5	4.0	24.75	3
J1021+0519	10 21 31.48	+05 19 00.9	G	0.1562	II	13.9	2.23	17.439	167.5	5.0	25.03	3
J1024+3647	10 24 43.08	+36 47 20.9	G	0.3190	II	2.9	0.79	20.335	132.3	4.0	25.62	44
J1027–2312	10 27 54.87	−23 12 03.4	Q	0.3090	II	3.3	0.89	18.376	578.5	17.4	26.22	38
J1030+5310	10 30 50.91	+53 10 28.7	Q	1.1975	II	1.7	0.84	18.013	55.6	1.7	26.60	48
J1032+2756	10 32 14.02	+27 56 01.7	G	0.0852	II	11.0	1.04	16.874	276.7	8.8	24.68	26
J1032+5644	10 32 58.90	+56 44 53.4	G	0.0453	I	35.0	1.83		481.8	14.8	24.35	40
J1036+3831	10 36 22.99	+38 31 30.7	G	0.3408	II	3.1	0.89	19.327	132.2	4.0	25.68	44
J1047+7419	10 47 54.49	+74 19 35.6	G	0.1210	II	11.2	1.45	16.592	59.1	2.9	24.34	26
J1048+1108	10 48 43.44	+11 08 02.4	G	0.1570	II	4.9	0.79	17.312	219.0	6.6	25.15	3
J1049–1308	10 49 45.73	−13 08 14.6	G	(0.15)	II	5.3	0.82	17.532	191.0	5.7	25.05	3
J1054+4152	10 54 03.27	+41 52 57.6	Q	1.0912	II	4.7	2.31	18.297	13.9	0.4	25.90	25
J1054+0227	10 54 21.16	+02 27 55.0	G	(0.34)	II	2.5	0.71	18.986	314.6	9.4	26.05	2
J1056+4100	10 56 36.26	+41 00 41.3	Q	1.7863	II	1.5	0.77	19.878	17.0	0.5	26.49	25
J1058+0810	10 58 17.69	+08 10 59.6	G	(0.33)	II	6.1	1.73	20.823	45.9	1.4	25.19	3
J1058+5140	10 58 17.89	+51 40 17.7	G	0.4150	II	4.5	1.48	20.035	59.5	1.8	25.53	23
J1058+2445	10 58 38.67	+24 45 35.1	G	(0.201)	II	10.4	2.13	18.809	147.0	12.0	25.21	4
J1059–1709	10 59 20.07	−17 09 22.6	G	0.1027	II	11.5	1.33	16.105	154	7.0	24.60	4
J1101+3634	11 01 09.46	+36 34 30.0	G	0.7500	II	2.5	1.10		124.0	3.9	26.46	44
J1101–1053	11 01 44.94	−10 53 18.7	G	(0.15)	II	14.2	2.21	17.948	98.4	3.0	24.76	3
J1101+4649	11 01 47.56	+46 49 10.4	G	0.6808	II	2.2	0.92	22.031	73.2	2.2	26.13	44
J1108+0202	11 08 45.49	+02 02 40.9	Q	0.1574	II	9.3	1.50	17.372	980.7	29.4	25.81	3
J1111+2657	11 11 25.21	+26 57 48.9	G	0.0335	I	28.7	1.12	15.543	135.8	4.1	23.55	57
J1113+4017	11 13 05.54	+40 17 29.8	G	0.0745	I/II	12.0	1.01	15.839	235.1	7.5	24.50	26
J1126–0042	11 26 03.33	−00 42 41.3	G	0.3320	II	4.0	1.14	18.905	160.7	4.8	25.74	3
J1130–1320	11 30 19.90	−13 20 50.0	Q	0.6337	II	4.9	2.01	16.166	1134	34.1	27.24	58
J1130+0629	11 30 51.73	+06 29 53.3	G	0.3970	II	4.4	1.41	19.785	232.3	7.0	26.08	1,2
J1145–0033	11 45 53.66	−00 33 04.5	Q	2.0522	II	2.6	1.34	19.628	24.2	0.7	26.79	59
J1147+3501	11 47 22.13	+35 01 07.5	G	0.0631	II	11.8	0.85	15.447	842.0	25.4	24.89	26
J1148–0404	11 48 55.88	−04 04 09.6	Q	0.3410	II	3.2	0.93	18.371	612.9	18.5	26.35	60
J1151+3355	11 51 39.68	+33 55 41.8	Q	0.8481	II	2.1	0.97	18.207	65.2	2.0	26.31	25
J1155+4029	11 55 49.54	+40 29 40.2	G	(0.53)	II	3.8	1.43	21.635	317.6	9.6	26.51	46
J1200+3449	12 00 50.48	+34 49 20.9	G	(0.50)	II	2.5	0.91	21.517	234.0	7.2	26.32	46

Table 1 continued

IAU name (1)	α (2000) (h m s) (2)	δ (2000) (° ' '') (3)	ID (4)	z (5)	FR type (6)	LAS arcmin (7)	D (Mpc) (8)	r (mag) (9)	S_I (mJy) (10)	δS_I (mJy) (11)	$\log P_{tot}$ W/Hz (12)	Ref. (13)
J1208+0259	12 08 17.53	+02 59 16.5	G	0.2410	II	3.5	0.73	19.536	47.9	2.8	24.90	1
J1211+7419	12 11 58.68	+74 19 04.1	G	0.1076	II	8.1	0.94	16.535	625.1	18.9	25.25	61
J1213-0500	12 13 32.87	-05 00 24.1	G	0.0860	II	8.9	0.85	17.215	55.7	1.7	23.99	3
J1216+4159	12 16 09.60	+41 59 28.3	Q	0.2426	II	5.2	1.19	18.350	401.5	12.5	25.83	26
J1216+6724	12 16 37.24	+67 24 41.4	G	0.3616	II	5.8	1.75	19.365	181.2	5.7	25.88	37
J1220+6341	12 20 36.41	+63 41 44.4	G	0.1876	II	4.7	0.88	17.785	255.0	7.9	25.39	62
J1229+3555	12 29 25.53	+35 55 32.1	Q	0.8328	II	1.7	0.78	19.375	54.2	1.6	26.20	25
J1232-1015	12 32 15.90	-10 15 25.6	G	0.2531	II	8.6	1.98	18.344	302.6	15.4	25.75	1
J1234+5318	12 34 58.46	+53 18 51.3	G	(0.642)	II	10.8	4.45	20.690	114.8	6.1	26.26	26
J1235+3925 ^m	12 35 04.75	+39 25 38.1	G	3.2200	II	2.2	1.01		260.1	8.0	28.27	63
J1235+2120	12 35 26.67	+21 20 34.8	G	0.4227	II	2.5	0.83	19.990	2911	87.4	27.24	21
J1236+1034	12 36 04.52	+10 34 49.3	Q	0.6671	II	1.7	0.71	17.620	222.7	6.7	26.59	25
J1242+3838	12 42 36.82	+38 38 06.1	G	0.4077	II	2.3	0.74	20.415	31.9	1.0	25.24	64
J1247+6723	12 47 33.33	+67 23 16.5	G	0.1073	II	11.6	1.35	16.876	356.7	10.9	25.00	26
J1251+7537	12 51 05.99	+75 37 38.9	G	0.1970	II	4.0	0.78	17.936	86.7	3.0	24.96	37
J1251+5034	12 51 42.03	+50 34 24.7	G	0.5490	II	2.3	0.88	19.990	1175	35.2	27.11	65
J1253-0139	12 53 09.09	-01 39 39.9	G	(0.24)	II	3.9	0.88		176.2	5.3	25.46	3
J1253+4041	12 53 12.28	+40 41 24.6	G	0.2295	I/II	4.6	1.01	18.090	38.2	1.8	24.75	45
J1254+2933	12 54 34.05	+29 33 41.0	G	0.5290	II	4.9	1.84	20.443	41.4	1.9	25.62	46
J1256+3638	12 56 13.90	+36 38 29.1	G	0.4685	II	2.6	0.90	19.986	145.3	4.4	26.04	44
J1259-7737	12 59 09.00	-77 37 28.4	G	(>0.3)	II	5.7	>1.51		439.0 ^c	13.2	25.90	12
J1301+5105	13 01 25.90	+51 05 00.7	G	(0.275)	II	10.3	2.57	19.050	18.7	2.8	24.62	23
J1304+2454	13 04 51.42	+24 54 45.9	Q	0.6025	II	2.4	0.97	17.497	45.0	1.4	25.79	25
J1304-3249	13 04 58.53	-32 49 15.9	G	0.1530	II	6.0	0.95		1530	46.0	25.97	21
J1308+6154	13 08 44.75	+61 54 15.3	G	0.1626	II	8.9	1.48	17.642	94.9	3.5	24.81	26
J1311-4422	13 11 23.76	-44 22 41.2	G	0.0506	I/II	14.4	0.85		1119 ^b	35.5	24.83	66
J1311+4058	13 11 43.09	+40 58 59.8	G	0.1106	II	6.2	0.74	17.225	594.3	18.0	25.25	67
J1312+4450	13 12 17.00	+44 50 21.3	G	0.0356	I	22.6	0.96	15.151	278.4	8.6	23.91	26
J1313+6937	13 13 58.86	+69 37 18.2	G	0.1060	II	7.1	0.82	17.449	1433	43.1	25.60	62
J1321+3741	13 21 06.64	+37 41 53.5	Q	1.1390	II	1.5	0.74	18.776	63.8	1.9	26.60	25
J1326+4934	13 26 14.34	+49 34 31.5	G	(0.42)	II	2.8	0.93	19.615	674.9	20.3	26.60	21
J1327+5749	13 27 41.32	+57 49 43.4	G	0.1202	II	12.1	1.61	16.390	89.0	4.0	24.51	4
J1327+1748	13 27 43.50	+17 48 37.5	G	0.6569	II	2.0	0.84	21.139	70.0	12.0	26.07	4
J1328-0129	13 28 34.15	-01 29 17.6	G	0.1513	II	5.4	0.85	17.613	335.2	10.1	25.30	3
J1328-0307	13 28 34.37	-03 07 44.8	G	0.0854	II	13.4	1.28	17.752	214.2	7.0	24.57	45
J1330+1826	13 30 12.44	+18 26 06.8	Q	0.2592	II	3.5	0.84	18.368	12.5	0.5	24.39	50
J1330+3850	13 30 36.19	+38 50 19.7	G	0.6300	II	4.7	1.93	19.375	22.5	1.4	25.54	46
J1334-1009	13 34 18.56	-10 09 29.0	G	0.0838	II	13.7	1.24	16.564	1878	56.4	25.47	68

Table 1 continued

IAU name (1)	α (2000) (h m s) (2)	δ (2000) (° ' '') (3)	ID (4)	z (5)	FR type (6)	LAS arcmin (7)	D (Mpc) (8)	r (mag) (9)	S_I (mJy) (10)	δS_I (mJy) (11)	$\log P_{tot}$ W/Hz (12)	Ref. (13)
J1335–8018	13 35 59.70	−80 18 05.1	G	0.2478	II	10.1	2.34		483.0 ^c	14.5	25.75	12
J1340+4232	13 40 34.70	+42 32 32.2	Q	1.3424	II	2.3	1.17	18.929	21.6	0.7	26.30	25
J1342+3758	13 42 54.54	+37 58 18.1	G	0.2270	II	11.3	2.45	18.304	104.9	3.5	25.18	45
J1344+3317	13 44 15.75	+33 17 19.1	Q	0.6868	II	2.4	1.04	19.186	149.5	4.5	26.45	2
J1345+5403	13 45 57.56	+54 03 16.6	G	0.1626	II	4.8	0.80	17.960	340.3	10.5	25.38	21
J1350–1634	13 50 36.14	−16 34 49.5	Q	0.0977	II	11.1	1.19	16.849	299.6	9.0	24.84	2
J1350+6429	13 50 42.04	+64 29 30.6	G	0.7100	II	2.2	0.95	20.864	2036	61.1	27.62	69
J1353+2631	13 53 35.92	+26 31 47.5	Q	0.3079	II	2.6	0.71	17.488	244.6	7.3	25.85	21
J1354–0705	13 54 18.21	−07 05 27.1	G	(0.19)	II	4.0	0.75	18.947	97.9	2.9	24.98	3
J1355+2923	13 55 17.61	+29 23 33.9	G	0.5010	II	4.4	1.61	20.422	123.0	3.9	26.04	46
J1400+3019	14 00 43.43	+30 19 18.7	G	0.2060	II	10.9	2.19	18.117	446.8	13.7	25.72	70
J1408+3054	14 08 06.21	+30 54 48.4	Q	0.8413	II	3.7	1.69	17.322	30.1	0.9	25.96	71
J1409–0302	14 09 48.86	−03 02 32.6	G	0.1378	II	9.5	1.37	17.452	164.0	4.9	24.90	72
J1410+2955	14 10 36.80	+29 55 50.9	Q	0.5740	II	2.5	0.98	18.540	16.4	0.5	25.30	25
J1411+0619	14 11 09.74	+06 19 45.6	G	0.3590	II	5.2	1.56	19.805	110.5	3.3	25.65	3
J1412+4212	14 12 44.10	+42 12 57.7	Q	0.8046	II	1.7	0.78	19.887	89.9	2.7	26.39	44
J1418+3746	14 18 37.65	+37 46 24.5	G	0.1349	II	7.7	1.09	17.099	51.8	3.4	24.38	26
J1420–0545	14 20 23.80	−05 45 28.8	G	0.3067	II	17.4	4.69	19.811	95.5	2.9	25.44	73
J1421+4144	14 21 05.61	+41 44 48.5	G	0.3670	II	3.2	0.97	19.275	3177	95.3	27.14	63
J1427+2632	14 27 35.61	+26 32 14.5	Q	0.3638	II	4.0	1.21	16.409	367.3	11.2	26.19	21
J1428+2918	14 28 19.24	+29 18 44.2	G	0.0870	II	14.7	1.42	16.411	430.7	13.4	24.89	26
J1428+3938	14 28 45.98	+39 38 42.2	G	(0.50)	II	4.5	1.64	20.812	86.8	3.1	25.88	46
J1429+0715	14 29 55.38	+07 15 12.9	G	0.0548	I	11.2	0.71	15.452	1969	59.2	25.14	74
J1432+1548	14 32 15.54	+15 48 22.4	Q	1.0159	II	2.8	1.36	18.456	165.9	5.2	26.90	60,75
J1435+4948	14 35 10.30	+49 48 19.4	Q	0.1661	II	5.0	0.84	17.461	36.0	1.1	24.42	76
J1436–1613	14 36 49.61	−16 13 41.0	Q	0.1445	I/II	10.3	1.55	15.803	235.2	9.8	25.10	77
J1445+3051	14 45 27.05	+30 51 28.9	G	0.4169	II	5.0	1.65	19.068	142.9	4.7	25.92	46
J1445–0540	14 45 56.35	−05 40 56.7	G	0.3670	II	7.0	2.13	20.117	239.6	7.2	26.01	3
J1448–4008	14 48 51.01	−40 08 45.7	G	0.1230	II	11.5	1.54		48.0		24.26	78,79
J1450+1006	14 50 49.40	+10 06 49.1	G	0.0545	I/II	39.0	2.47	16.698	137.5	5.2	23.98	80
J1451+3357	14 51 33.58	+33 57 42.8	G	0.3251	II	4.1	1.15		131.3	4.3	25.63	46
J1453+3308	14 53 02.86	+33 08 42.4	G	0.2482	II	5.6	1.30	18.365	450.7	13.5	25.90	26,64,81
J1457–0613	14 57 47.12	−06 13 18.0	G	0.1671	II	4.2	0.71	19.591	465.3	14.0	25.53	3
J1459–0432	14 59 57.24	−04 32 29.8	G	(0.27)	II	6.8	1.68	19.239	61.3	1.8	25.12	3
J1504+6856	15 04 12.77	+68 56 12.8	Q	0.3180	II	3.1	0.87	17.578	458.2	13.7	26.15	2,37
J1507+0234	15 07 03.78	+02 34 07.2	G	0.1238	II	6.3	0.83	17.856	38.0	2.5	24.17	29
J1511+0751	15 11 00.01	+07 51 50.0	G	0.4594	II	2.2	0.76	19.380	1175	35.2	26.93	82
J1513+3841	15 13 29.65	+38 41 57.3	G	(0.52)	II	4.5	1.68	19.041	18.2	1.3	25.25	48

Table 1 continued

IAU name (1)	α (2000) (h m s) (2)	δ (2000) (° ' '') (3)	ID (4)	z (5)	FR type (6)	LAS (arcmin) (7)	D (Mpc) (8)	r (mag) (9)	S_I (mJy) (10)	δS_I (mJy) (11)	$\log P_{tot}$ W/Hz (12)	Ref. (13)
J1520–0546	15 20 13.29	−05 46 27.0	G	0.0605	II	22.0	1.53	16.485	26.8	0.8	23.37	3
J1521+5105	15 21 14.55	+51 05 00.9	G	(0.37)	II	4.3	1.31	19.139	1198	36.0	26.72	65
J1525+3345	15 25 00.79	+33 45 42.4	G	(0.47)	II	3.6	1.27	20.974	44.9	2.0	25.54	46
J1536+8423	15 36 57.27	+84 23 10.8	G	0.2010	II	7.9	1.56	18.989	368.0	11.3	25.61	26
J1540–0127	15 40 56.80	−01 27 10.0	G	0.1490	II	4.9	0.76	17.679	194.1	5.8	25.05	3
J1543–0112	15 43 11.95	−01 12 46.6	G	0.3680	II	2.9	0.88	19.977	114.3	3.4	25.69	3
J1548–3216	15 48 58.05	−32 16 57.6	G	0.1082	II	8.3	0.97		1772	53.3	25.71	18
J1552+2005	15 52 09.19	+20 05 23.2	G	0.0890	II	19.6	1.95	17.353	2384	71.6	25.67	14
J1554+3945	15 54 26.85	+39 45 08.7	G	(0.35)	II	3.7	1.09	19.997	69.3	2.5	25.43	46
J1555+3653	15 55 00.39	+36 53 37.4	G	0.2472	II	5.8	1.34	18.891	100.9	3.5	25.25	46
J1604+3731	16 04 23.44	+37 31 49.3	G	0.8140	II	2.9	1.32		117.0	3.8	26.52	44
J1604+3438	16 04 45.89	+34 38 16.5	G	0.2817	II	3.3	0.84	19.611	139.6	4.5	25.52	46
J1615+3826	16 15 52.23	+38 26 31.9	G	0.1856	II	4.4	0.81	17.942	27.0	1.5	24.40	46
J1616+4825	16 16 01.26	+48 25 35.4	G	(0.233)	II	12.3	2.71	18.954	73.5	4.3	25.05	26
J1628+5146	16 28 04.06	+51 46 31.4	G	0.0560	II	18.4	1.19	16.085	628.8	19.1	24.66	83
J1632+8232	16 32 31.97	+82 32 16.4	G	0.0247	I/II	52.0	1.56		2100	63.1	24.46	18
J1635+3608	16 35 22.54	+36 08 04.9	G	0.1650	I/II	5.3	0.90	17.731	95.1	3.3	24.83	46
J1637+4146	16 37 53.38	+41 46 01.4	G	0.8670	II	2.2	1.02		64.7	2.3	26.33	44
J1649+3114	16 49 06.12	+31 14 31.4	G	0.4373	II	3.5	1.18	19.261	146.8	4.7	25.98	46
J1702+4217	17 02 55.95	+42 17 48.8	G	0.4760	II	3.0	1.07	21.780	181.6	5.7	26.16	44
J1706+4340	17 06 25.44	+43 40 40.2	Q/G	(0.525)	II	2.0	0.75	19.743	148.0	4.4	26.17	84
J1712+3558	17 12 24.87	+35 58 26.2	G	0.3357	II	3.5	1.00	20.025	82.6	2.9	25.46	46
J1723+3417	17 23 20.80	+34 17 58.0	Q	0.2060	II	4.1	0.82	16.043	1639	49.2	26.28	38
J1725+3923	17 25 17.05	+39 23 05.3	G	0.2898	II	4.8	1.24	22.008	78.8	3.0	25.30	46
J1728–7237	17 28 28.10	−72 37 34.9	G	0.4735	II	6.2	2.20		214.0 ^c	6.4	26.05	12
J1738+3733	17 38 20.93	+37 33 33.8	G	0.1562	II	6.5	1.04	17.419	235.5	7.3	25.17	26
J1745+7115	17 45 43.53	+71 15 48.7	G	0.2160	II	4.4	0.92	18.805	887.5	26.7	26.06	37
J1748–2335	17 48 39.05	−23 35 21.2	G	0.2400	II	5.7	1.29		398.5	12.0	25.81	78,85
J1815+6531	18 15 11.79	+65 31 21.9	G	0.9600	II	2.1	1.00		149.8	4.7	26.71	86,87
J1815+6818	18 15 29.52	+68 18 30.5	G	0.7940	II	3.3	1.49	21.081	195.8	6.1	26.72	86,87
J1835+6635	18 35 07.30	+66 35 00.0	G	0.3540	II	4.4	1.31	19.331	136.7	4.5	25.73	37
J1835+6204	18 35 10.92	+62 04 08.1	G	0.5194	II	3.8	1.42	20.013	794.5	23.9	26.88	88
J1838+6555	18 38 11.54	+65 55 02.6	Q	0.2300	II	6.8	1.49	16.638	454.6	22.8	25.83	26,89
J1844+6522	18 44 07.41	+65 22 03.1	G	0.1970	II	7.5	1.45	18.308	98.0	3.6	25.01	37
J1853+5046	18 53 32.51	+50 46 07.3	G	0.0958	II	7.0	0.74	16.566	126.5	4.4	24.45	26
J1853+8002	18 53 51.07	+80 02 42.5	G	0.2139	II	5.6	1.16	19.994	153.9	5.0	25.29	37
J1910–7049	19 10 55.20	−70 49 00.9	G	0.2152	II	6.0	1.25		238.0 ^c	7.1	25.31	12
J1918+7415	19 18 34.89	+74 15 05.1	G	0.1940	II	6.6	1.26	18.179	571.7	17.3	25.77	37

Table 1 continued

IAU name (1)	α (2000) (h m s) (2)	δ (2000) ($^{\circ}$ ' $''$) (3)	ID (4)	z (5)	FR type (6)	LAS arcmin (7)	D (Mpc) (8)	r (mag) (9)	S_I (mJy) (10)	δS_I (mJy) (11)	$\log P_{tot}$ W/Hz (12)	Ref. (13)
J1919–7959	19 19 13.86	−79 59 06.7	G	0.3460	II	6.1	1.78	19.622	1262 ^c	37.9	26.50	18
J1919+5143	19 19 22.75	+51 43 33.9	Q	0.2840	II	7.3	1.86		385.3	11.8	25.96	26
J1920+4526	19 20 01.66	+45 26 52.9	G	0.0522	II	16.7	1.01	15.340	287.9	14.9	24.26	26
J1921+4806	19 21 13.97	+48 06 18.7	G	0.1023	I	13.5	1.52	16.489	1032	51.7	25.42	26
J1946–8222	19 46 50.50	−82 22 53.8	G	0.3330	II	7.4	2.11		219.0 ^c	6.6	25.70	12
J1951+7037	19 51 40.82	+70 37 40.0	G	0.5500	II	5.2	2.00	20.825	92.3	3.2	26.01	37
J2008+0049	20 08 43.37	+00 49 18.9	G	(0.412)	II	11.0	3.71	20.526	81.0	3.0	25.66	4
J2018–5539	20 18 01.31	−55 39 30.8	G	0.0606	I	20	1.37		2653 ^b	80.9	25.35	66,90
J2034–2630	20 34 49.23	−26 30 36.4	G	0.1033	II	6.7	0.78	16.547	76.0	6.0	24.30	4
J2035+6805	20 35 16.55	+68 05 41.6	G	0.1330	I	11.5	1.61	18.568	253.7	8.1	25.06	37
J2042+7508	20 42 37.31	+75 08 02.4	Q	0.1040	II	10.2	1.16	14.576	1789	53.7	25.68	91
J2059+6247	20 59 09.56	+62 47 44.1	G	0.2670	II	4.7	1.15	20.262	107.7	3.6	25.35	37
J2059+2434	20 59 39.81	+24 34 23.9	G	(0.116)	II	8.2	1.06	17.740	149.0	8.0	24.70	4
J2103+6456	21 03 13.87	+64 56 55.3	G	0.2150	II	4.8	1.00	20.100	118.3	4.0	25.18	37
J2145+8154	21 45 30.90	+81 54 53.7	G	0.1457	II	18.3	2.78	17.753	395.4	12.2	25.34	26
J2159–7219	21 59 09.99	−72 19 01.1	G	0.0970	II	9.2	0.98		142.0 ^c	4.3	24.34	12
J2219–2021	22 19 44.23	−20 21 30.6	G	1.1480	II	1.5	0.73		407.6	12.2	27.42	6
J2230–3942	22 30 40.28	−39 42 52.1	Q	0.3181	II	3.3	0.91		591.1	17.7	26.26	2
J2233+1315	22 33 01.30	+13 15 02.5	G	(0.093)	II	16.0	1.71	16.504	125.0	4.0	24.42	4
J2234–0224	22 34 58.76	−02 24 18.9	Q	0.5500	II	3.3	1.27	18.333	75.7	2.3	25.92	3
J2239–0133	22 39 59.34	−01 33 51.4	G	0.0881	II	20.4	1.97	16.666	135.0	4.1	24.39	3
J2242+6212	22 42 32.13	+62 12 17.6	G	0.1880	II	4.2	0.78	21.896	288.7	8.8	25.44	37
J2245–0032	22 45 20.76	−00 32 06.1	G	(0.66)	II	3.0	1.25	22.018	17.0	0.6	25.46	23
J2250+2844	22 50 39.16	+28 44 45.5	G	(0.097)	II	8.4	0.93	16.747	120.0	9.0	24.44	4
J2253–3455	22 53 36.03	−34 55 30.8	G	0.2115	II	4.5	0.93		291.3	8.7	25.56	2
J2253–5812	22 53 58.98	−58 12 49.4	G	0.1764	II	4.3	0.76		5.4	0.2	23.65	12
J2256–3617	22 56 15.08	−36 17 59.1	G	0.0902	II	14.5	1.51		195.0	11.0	24.58	4
J2257–0052	22 57 34.43	−00 52 31.8	G	0.5220	II	5.3	1.98	20.790	80.2	3.0	25.89	9
J2304–1050	23 04 44.81	−10 50 47.7	G	0.2103	I	4.0	0.82	17.544	67.8	2.7	24.92	4,92
J2306–0930	23 06 32.18	−09 30 20.6	G	0.1593	I	6.2	1.01	17.519	136.9	4.5	24.96	93
J2312+1356	23 12 01.27	+13 56 55.9	G	0.1404	II	11.4	1.74	16.520	338.0	26.0	25.23	4
J2312+1845	23 12 07.57	+18 45 41.4	G	0.4265	II	3.4	1.14	20.006	1957	58.7	27.08	94
J2316–2823	23 16 00.58	−28 23 52.8	G	0.2293	II	8.7	1.89	17.925	296.2	15.1	25.64	2,5
J2316–0102	23 16 20.15	−01 02 07.3	Q	(0.221)	II	6.8	1.50	19.409	90.0	5.0	25.09	4
J2320–1320	23 20 13.98	−13 20 57.9	G	0.3927	II	4.0	1.11	19.591	330.2	16.6	26.22	1
J2321–2724	23 21 13.79	−27 24 48.6	G	0.2370	II	4.7	1.06	17.731	38.9	1.2	24.79	24
J2326+2458	23 26 23.20	+24 58 40.4	G	0.2549	II	11.7	2.88	18.676	274.0	27.0	25.71	4
J2328–0825	23 28 50.02	−08 25 11.8	G	0.3840	II	4.6	1.40	19.664	64.9	3.7	25.49	1,4

Table 1 continued

IAU name (1)	α (2000) (h m s) (2)	δ (2000) ($^{\circ}$ ' $''$) (3)	ID (4)	z (5)	FR type (6)	LAS arcmin (7)	D (Mpc) (8)	r (mag) (9)	S_I (mJy) (10)	δS_I (mJy) (11)	$\log P_{tot}$ W/Hz (12)	Ref. (13)
J2333–2343	23 33 55.24	–23 43 40.7	G	0.0477	II	18.9	1.05	16.321	1167	35.1	24.78	2
J2335+5215	23 35 52.14	+52 15 38.6	G	0.0706	II	10.2	0.85	16.461	95.0	8.0	24.05	4
J2344–0032	23 44 40.04	–00 32 31.7	Q	0.5014	II	2.7	0.99	17.669	34.9	1.1	25.49	25
J2345–0449	23 45 32.70	–04 49 25.4	G	0.0756	II	17.1	1.46	15.968	173.9	5.2	24.38	3
J2355+7955	23 55 23.33	+79 55 19.6	G	1.3360	II	1.4	0.71		1722	51.7	28.20	95
J2355+0256	23 55 31.63	+02 56 07.1	G	(0.657)	II	8.1	3.48	20.619	80.0	9.0	26.13	4
J2356–0131	23 56 06.40	–01 31 51.4	Q	1.0280	II	1.7	0.81	20.820	225.6	6.8	27.02	21
J2359–6054	23 59 04.36	–60 54 59.3	G	0.0963	II	7	0.74		26240	460	26.77	41

Column description: (1) – source name, (2) and (3) – J2000.0 coordinates of the host optical object, (4) – optical identification (G – galaxy or Q – quasar), (5) – redshift, (6) – radio morphological type, (7) – angular size in arcmin, (8) projected linear size in Mpc, (9) – optical aperture magnitude in r band, (10) total flux-density at 1.4 GHz, unless indicated, in units of mJy , (11) – error of flux-density in mJy, (12) – total radio luminosity at 1.4 GHz in units of W/Hz (14) – references.

Notes: (a) – flux-density at 1.388 GHz from Saripalli et al. (2012), (b) – SUMSS measurement of flux-density, (c) – flux-density at 0.843 GHz from Saripalli et al. (2005), (d) – flux-density at 0.325 GHz from Sebastian et al. (2018), (r) – optical r magnitudes taken from Saripalli et al. (2012). The redshifts given in brackets are photometric, (n) – in Weżgowiec, Jamrozy & Mack (2016) the diffuse radio emission can be seen. It extends for \sim 23' and it is presumably the evidence of past radio emission, (m) – GRG proposed by Mack et al. (2005). Its size is uncertain, (p) – we also found different value of photometric redshift equal to 0.473 (Brescia, Cavuoti & Longo 2015).

References: 1. Bankowicz et al. (2015), 2. Proctor (2016), 3. Machalski, Koziel-Wierzbowska & Jamrozy (2007), 4. Dabhade et al. (2017), 5. Solovyov & Verkhodanov (2014), 6. Kapahi et al. (1998), 7. Saripalli et al. (2012), 8. Subrahmanyam et al. (2010), 9. Sadler, Cannon & Mauch (2007), 10. Saikia, Konar & Kulkarni (2006), 11. Santiago-Bautista et al. (2016), 12. Saripalli et al. (2005), 13. Djorgovski et al. (1995), 14. Mack et al. (1997), 15. Andernach et al. (1992), 16. van Breugel & Jägers (1982), 17. Laing, Riley & Longair (1983), 18. Subrahmanyam, Saripalli & Hunstead (1996), 19. Lacy (2000), 20. Colafrancesco et al. (2016), 21. Nilsson (1998), 22. Fomalont et al. (1978), 23. Rentería Macario & Andernach (2017), 24. Sadler et al. (2002), 25. Kuźmicz & Jamrozy (2012), 26. Schoenmakers et al. (2001), 27. Tamhane et al. (2015), 28. Simpson et al. (2006), 29. Koziel-Wierzbowska & Stasińska (2011), 30. de Bruyn (1989), 31. Schoenmakers et al. (1998), 32. Saripalli, Subrahmanyam & Hunstead (1994), 33. Hunik & Jamrozy (2016), 34. Reid, Kronberg & Perley (1999), 35. Hurley-Walker et al. (2015), 36. Amirkhanyan, Afanasiev & Moiseev (2015), 37. Lara et al. (2001b), 38. Ishwara-Chandra & Saikia (1999), 39. Filipovic et al. (2013), 40. Jägers (1986), 41. Malarecki et al. (2015), 42. Saripalli, Gopal-Krishna & Kuehr (1986), 43. Kronberg, Wielebinski & Graham (1986), 44. Cotter, Rawlings & Saunders (1996), 45. Machalski, Jamrozy & Zola (2001), 46. Machalski et al. (2006), 47. Hes, de Vries & Barthel (1995), 48. Kuligowska et al. (2009), 49. Lacy et al. (1993), 50. Coziol et al. (2017), 51. Sebastian et al. (2018), 52. Kuligowska et al. (2009), 53. Law-Green et al. (1995), 54. Proctor (2011), 55. Högbom (1979), 56. Machalski & Condon (1999), 57. Owen et al. (2000), 58. Bhatnagar, Krishna & Wisotzki (1998), 59. Kuźmicz, Kuligowska & Jamrozy (2011), 60. Hintzen, Ulvestad & Owen (1983), 61. van Breugel & Willis (1981), 62. Saunders, Baldwin & Warmer (1987), 63. Mack et al. (2005), 64. Schoenmakers et al. (2000a), 65. Machalski (1998), 66. Jones & McAdam (1992), 67. Djorgovski et al. (1990), 68. Saripalli et al. (1997), 69. McCarthy et al. (1997), 70. Parma et al. (1996), 71. Gregg, Becker & de Vries (2006), 72. Hota et al. (2011), 73. Machalski et al. (2008), 74. Falco et al. (1999), 75. Singal, Konar & Saikia (2004), 76. Andernach et al. (2012), 77. Bassani et al. (2016), 78. Masetti, Parisi & Palazzi (2013), 79. Molina et al. (2015), 80. Clarke et al. (2017), 81. Konar et al. (2006), 82. Baum & Heckman (1989), 83. Röttgering et al. (1996), 84. Marecki, Jamrozy & Machalski (2016), 85. Molina et al. (2014), 86. Lacy et al. (1999), 87. Lacy, Rawlings & Warner (1992), 88. Lara et al. (1999), 89. Hagen, Engels & Reimers (1999), 90. Saripalli et al. (2008), 91. Riley et al. (1989), 92. Jones et al. (2009), 93. Best et al. (2005), 94. Leahy & Perley (1991), 95. Kharb, O'Dea & Baum (2008).